LA-UR-22-22458
Approved for public release; distribution is unlimited.

Title: Methodology for Determining Impulse and Quasi-Static Pressure Loading for Design of 6-ft Inner Diameter Confinement Vessel

Author(s): Rodriguez, Edward A.

Intended for: Report

Issued: 2022-03-15

Los Alamos National Laboratory, an affirmative action/equal opportunity employer, is operated by Triad National Security, LLC for the National Nuclear Security Administration of U.S. Department of Energy under contract 89233218CNA000001. By approving this article, the publisher recognizes that the U.S. Government retains nonexclusive, royalty-free license to publish or reproduce the published form of this contribution, or to allow others to do so, for U.S. Government purposes. Los Alamos National Laboratory requests that the publisher identify this article as work performed under the auspices of the U.S. Department of Energy. Los Alamos National Laboratory strongly supports academic freedom and a researcher's right to publish; as an institution, however, the Laboratory does not endorse the viewpoint of a publication or guarantee its technical correctness.

Los Alamos NATIONAL LABORATORY

J Division, Mail Stop P942, Los Alamos, NM 87545

RPT-SCE-21-2903, Rev. C

Methodology for Determining Impulse and Quasi-Static Pressure Loading for Design of 6-ft Inner Diameter Confinement Vessels

10 March 2022

Preparer

J-2	Edward A. Rodriguez	110240	EDWARD RODRIGUEZ (Affiliate)	Digitally signed by EDWARD RODRIGUEZ (Affiliate) Date: 2022.03.11 10:19:25 -07'00'
Org	*Name*	*Z#*	*Signature*	*Date*

Reviewers

J-2	Thomas A. Duffey	085879	Thomas Duffey	3/11/22
Org	*Name*	*Z#*	*Signature*	*Date*
J-2	Kevin R. Fehlmann	327402	KEVIN FEHLMANN (Affiliate)	Digitally signed by KEVIN FEHLMANN (Affiliate) Date: 2022.03.11 12:32:11 -07'00'
Org	*Name*	*Z#*	*Signature*	*Date*
M-6	Andrew T. Barnes	346584	Andrew Thomas Barnes	Digitally signed by Andrew Thomas Barnes Date: 2022.03.11 12:56:01 -07'00'
Org	*Name*	*Z#*	*Signature*	*Date*

Approvers

J-2: RLM	Brandy Cox Royer	108030	Brandy Royer	Digitally signed by Brandy Royer Date: 2022.03.14 10:45:18 -06'00'
Org	*Name*	*Z#*	*Signature*	*Approval Date*
OSH-ISH	Joseph M. Lloyd	185984	Joseph M Lloyd	Digitally signed by Joseph M Lloyd Date: 2022.03.14 14:41:50 -06'00'
Org	*Name*	*Z#*	*Signature*	*Approval Date*

This document deemed

______**UNCLASSIFIED**________________________

by: Brandy Royer Digitally signed by Brandy Royer Date: 2022.03.14 10:45:05 -06'00'

LANL Derivative Classifier/**Signature and Date**

REVISION HISTORY

Revision	Date	Description of Change
A	11/30/21	Original issue
B	1/13/22	• Added Section 2.4, *Dynamic Regime for Vessel Design*; discussing vessel response under pressure-dominated and impulse-dominated behavior. • Also, included several paragraphs in the Executive Summary addressing *Dynamic Regime for Vessel Design*. • Added Section 5.2, *HMX-Based Explosive Comparison*, showing similar performance measures for peak reflected specific impulse and quasi-static gas pressure for HMX, LX-14 and PBX-9501. • Included a recommendation to use PBX-9501 as the base explosive for SCE applications in confinement vessels involving utilization of either LX-14 or PBX-9501.
C	3/14/22	Modified Section 4.0 into two sub-sections; • Section 4.1, Confinement Vessel Gas Pressure and • Section 4.2, U1a Facility Zero-Rooms, providing TNT-equivalence for O_2 rich atmospheres.

EXECUTIVE SUMMARY

A brief study of the TNT-equivalence of PBX-9501 is presented herein utilizing a new basis via application of one-dimensional spherical (1DS) hydrocode models in a 6-ft ID confinement vessel geometry with no internal furniture. Specifically, TNT-equivalence herein is based upon two separate features:

(1) matching the peak reflected specific impulse of PBX-9501 to TNT under detonation process, and

(2) matching quasi-static peak gas pressure of PBX-9501 to TNT at steady-state.

LANL (i.e., J-2) has been using a TNT-Equivalence for PBX-9501 in confinement vessel design that appears to be in conflict with the LLNL derived quantities using the thermochemical code CHEETAH. Differences between LANL and LLNL approach to TNT-equivalence have provided an impetus for this investigation. For both TNT and PBX-9501, 1D spherical hydrocode models have been developed under confined constant-volume conditions in 6-ft ID vessels with the use of CTH, as well as application of the thermochemical code CHEETAH.

Although the most widely used methodology for determining TNT-equivalence for HE detonations (as prescribed in UFC-3-340-02) is the product of the ratio of heat-of-detonation of the HE in question to that of TNT and the mass of HE in question, results of the 1D spherical hydrocode modeling provide a different answer. In other words, the ratio of heat-of-detonation has often been applied to a wide variety of problems, which leads to a constant single-valued (invariant) factor applied to the weight of the HE in question.

It is necessary to provide an important distinction to design of protective structures, such as confinement vessels, within the complete regime of dynamic loading; whether the design is based purely upon impulse-dominated, pressure-dominated loading or a mixed-mode regime. In other words, as described in UFC-3-340-02;

> *"A protective element subjected to high intensity shock pressures may be designed for the impulse rather than the pressure pulse, only if the duration of the applied pressure acting on the element is short in comparison to its response time. However, if the time to reach maximum displacement is equal to or less than three times the load duration, then a simplified pressure pulse representing the full pressure-time relationship should be used for these cases."*

Although protective elements subjected to high-explosive blast loading are generally designed to impulsive loads, it actually depends on the pulse duration and natural frequency of the structure (i.e., square-root of the ratio of structural stiffness to mass). The investigation conducted herein is limited to 6-ft diameter confinement vessels, for which a purely impulsive load is applicable. In general, the response time is long compared to the pulse duration, but both the pulse duration and response time should be calculated for each case to determine the appropriate design criteria. i.e., impulse-dominated vs. simplified pressure-dominated pulse.

Results presented herein provide the following conclusions:

1. Peak reflected specific impulse is the key to meaningful scaling of explosives for shock loading in a confined volume.
    a. The structural response of a confinement vessel is directly related to the driving energy supplied during the detonation; i.e., the peak reflected specific impulse.
    b. For the 6-ft ID confinement vessel geometry identified in this study, TNT-equivalence is shown to be approximately 1.188 for a 40-lb PBX-9501 charge.
    c. Both, CTH library JWL EOS and CHEETAH-derived JWL EOS were applied to hydrocode models, showing minor differences in overall results.
2. The importance of proper accounting for incomplete combustion when determining equivalent charge for quasi-static pressure.
    a. As shown in the foregoing analysis, the TNT-equivalence for quasi-static gas pressure without afterburn (i.e., vacuum) is approximately 1.49 for the given vessel geometry and the 40-lb PBX-9501 charge.
    b. CTH hydrocode models and CHEETAH constant-volume explosion calculations results agree within 5%.
3. Using a constant TNT-equivalence conversion factor between PBX-9501 and TNT, for either the shock loading or the quasi-static pressure, is not applicable to confinement vessels, i.e., constant-volume explosion applications.
4. Original differences between LANL and LLNL results for TNT-equivalence were based upon the diverse application of the TNT heat-of-detonation values, where LANL utilized UFC-3-340-02 values and LLNL uses thermochemical principles.
5. Comparison of CTH 1DS analyses for HMX, LX-14 and PBX-9501 for detonation event, and CHEETAH analyses for combustion events, shows minor differences in peak reflected pressure, and particularly peak reflected specific impulse, and peak quasi-static gas pressure. All three HMX-based high-explosives perform similarly with minor differences.

As a result of analyses contained herein, coupled with the above listed conclusions, LANL provides the following recommendations:

1. It is recommended that LANL and LLNL remove TNT-equivalency methodology for U1a SCE vessel design applications, and instead use PBX-9501 as the base explosive.
    a. For shock loading of the vessel structure, no TNT conversion factors will be utilized, thereby ensuring a one-to-one correspondence.
    b. Likewise, this change should mitigate any further confusion in vessel design, especially ensuring the proper quasi-static gas pressure is applied to o-ring seal and feedthroughs based on the actual explosive.

2. CHEETAH closed-volume explosion calculations shall be used to determine peak quasi-static gas pressures in a confinement vessel.
    a. CHEETAH has the capability of determining the peak quasi-static gas pressure as a function of the available oxidizer in the system (i.e., all reactants), resulting in partial or full-afterburn.
    b. Results can be validated through simple (i.e., less sophisticated) thermodynamic principles and application of BLAST-X or CONWEP.
3. For zero-room pressurization due to a hypothetical confinement vessel failure, for example a feedthrough blow-out, a combination of CHEETAH calculations and BLAST-X is recommended.
    a. CHEETAH can determine both, the internal gas pressure in the vessel for the given free-volume and an unconfined detonation in the zero-room.
    b. BLAST-X will further determine the rate of pressure increase in the zero-room as a function of time and available heat-transfer mechanisms. Blast-X can also be used to validate the results of the CHEETAH analysis.
4. For other facility design applications, a TNT-equivalence methodology is fully recommended, as described by J. Maienschein and as shown in UFC-3-340-02, which utilizes the product of the ratio of heat-of-combustion of the explosive in question to that of TNT and the mass of the explosive.
    a. The assumption is that the closed-volume facility is large enough to ensure an abundance of oxidizer (or a stoichiometric mixture) to adequately combust 100% of the reaction product fuels.
        i. Assuming an unconfined detonation in a facility room or drift, an upper-bound solution of peak quasi-static gas pressure is ensured.
    b. The resulting TNT-equivalence factor for PBX-9501 in a large closed-volume is approximately 0.645, given the respective heat-of-combustion of PBX-9501 and TNT.
    c. For this type of analysis, CHEETAH is recommended because it can model the actual mass of reactants (i.e., HE, oxidizer and inert gases) in determining the peak quasi-static pressure for partial or full-afterburn.
5. Based on the CTH and CHEETAH analyses results comparing HMX, LX-14 and PBX-9501 demonstrating similar detonation and combustion performance, LANL recommends using PBX-9501 as the base explosive for SCE applications in confinement vessels involving either LX-14 or PBX-9501.

Table of Contents

TABLE OF FIGURES

LIST OF TABLES

NOMENCLATURE & SYMBOLS

C-J	Chapman-Jouguet
CTH	SNL hydrodynamic code
EOS	Equation-of-state
HE	High-explosives
HMX	Cyclotetramethylenetetranitramine
JWL	Jones-Wilkins-Lee
LANL	Los Alamos National Laboratory
NNSS	Nevada National Security Site
PBX	Plastic bonded explosive
SCE	Subcritical Experiment
STP	Standard temperature and pressure
TNT	2,4,6-trinitrotoluene
ToA	Time of arrival
UFC	United Facilities Criteria
VCS	Vessel Confinement System

Mathematical & Greek Symbols

ΔH_C^o	Heat-of-combustion, (kcal/mole)
ΔH_D^o	Heat-of-detonation, (kcal/mole)
ΔH_F^o	Heat-of-formation, (kcal/mole)
P	Pressure, (psig)
$\rho_{o(Exp)}$	Theoretical maximum density of HE, (g/cm^3)
T	Temperature, (K)

1.0 PURPOSE

The objective of this study is to determine the appropriateness of the current TNT-equivalence factors proposed by Lawrence Livermore National Laboratory (LLNL) through application of their thermochemical equilibrium and kinetics code, CHEETAH, and TNT-equivalence factors used by Los Alamos National Laboratory as dictated contractually through UFC-3-340-02. A comparison of TNT-equivalent factors is developed herein by application of 1D spherical hydrocode models.

2.0 BACKGROUND

A brief background is provided to assist in deciphering the state of TNT-equivalence for SCE applications. This report does NOT provide an exhaustive assessment and it only deals with the TNT-equivalence determined specifically for blast loads generated in a constant-volume 6-ft ID confinement vessel. Brief synopsis on the following is provided below:

- TNT-equivalence data, testing and methods
- LANL approach to TNT-equivalence
- LLNL thermochemical approach
- A note on code of record and standards

2.1 TNT-Equivalence Data, Tests and Methods

Design manuals such as TM 5-855, TM 5-1300, DOE-TIC-11268, and UFC-3-340-02 contain listings of TNT-equivalent factors for numerous explosives used in the DOE and DoD communities. TNT-equivalence is a factor that when multiplied by the weight of known explosive, it results in a TNT charge weight that would produce the same observed effect as the known explosive. The primary reason for this approach is the abundance of design data based upon TNT testing, which is available to engineers through graphical representation of empirical and semi-empirical shock parameters or design equations. A major drawback to utilizing these TNT-equivalence factors from any of the design manuals is they are inconsistent, even among each other, and sometimes differ by more than 30-50%. There are a significant number of TNT-equivalence test processes, as well as analytical methods which all depend on a predetermined explosive effect being observed or quantified. Kinney and Graham, and Cooper describe numerous tests, such as:

- Sand Crush
- Trauzl Test (Lead Block)
- Ballistic Mortar
- Ballistic Pendulum
- Plate Dent
- Cylinder
- Air Blast

All of the above tests do not necessarily measure the same output property of the explosive. Each test, rather, is designed to observe some predetermined, empirically measured output effect. Theoretical concepts have also been developed (see Cooper, 1994). Several TNT-equivalence methods have been proposed such as the C-J pressure ratio,

$$W_{TNT} = \frac{P_{C-J(Exp)}}{P_{C-J(TNT)}} W_{Exp} \qquad \text{Eq. (2.1)}$$

or Cooper's method which takes the ratio of the squares of detonation velocities

$$W_{TNT} = \frac{D^2_{C-J(Exp)}}{D^2_{C-J(TNT)}} W_{Exp} \qquad \text{Eq. (2.2)}$$

Kinney and Graham also provide a description of the Berthelot method which directly relates the heat of detonation multiplied by moles of gas released per mole of explosive, and inversely proportional to the square of the molecular weight of explosive.

$$\%W_{TNT} = 840\left(\Delta n\right)\frac{-\Delta H_{Exp}}{\left(M_W\right)^2_{Exp}} W_{Exp} \qquad \text{Eq. (2.3)}$$

Lastly, the most widely used theoretical concept is ratio of heat-of-detonation for shock loading, which will be discussed below in Sections 2.2 and 2.3.

2.2 LANL Approach to TNT-Equivalence

LANL has consistently used the guidance in TM 5-1300 and its successor document, UFC-3-340-02, to determine the TNT equivalence of specific explosives. UFC-3-340-02 provides tables of standard detonation parameters for many explosives, including the heat-of-detonation (i.e., the difference in heats-of-formation between the reaction products and reactants). The UFC guidance provides a very simple linear relationship for the equivalent mass of a TNT charge. For example, the equation below is written for the equivalence between PBX-9501 and TNT, as the product of the ratio of heat-of-detonation of PBX-9501 to that of TNT, and the weight of PBX-9501.

$$W_{TNT} = \frac{\left(\Delta H_d\right)_{PBX-9501}}{\left(\Delta H_d\right)_{TNT}} W_{PBX-9501} \qquad \text{Eq. (2.4)}$$

UFC-3-340-02 reports the heat-of-detonation values directly from Dobratz, UCRL-52997, LLNL Explosives Handbook, which happen to coincide with the maximum theoretical values, not lower-bound experimental data. The published heat-of-detonation from UFC-3-340-02 for TNT is 5.90 kJ/g and for PBX-9501 is 6.65 kJ/g. Thus, using the simplified form above, the TNT-equivalence for shock loading becomes 1.127 as compared with LLNL value of 1.312 (see Table 1 below).

Additionally, UFC-3-340-02 states the following for peak quasi-static gas pressures:

> *"The data presented in Figure 2-152 and Figures 2-153 to 2-164 are for TNT only and must be extended to include other potentially mass-detonating materials. Similar to the shock pressures, only a limited amount of data is available regarding the TNT equivalency of confined explosions and in particular the effects produced on gas pressures."*

Thus, UFC-3-340-02 provides a simple TNT-equivalence means for determining peak quasi-static gas pressures given a specified charge-weight to free-volume ratio. In effect, this simple relationship supposedly accounts for the level of oxidizer in the free-volume such that a null, partial or full-afterburn may be determined.

$$W_{TNT} = \frac{\phi\left[\Delta H_{Exp}^{c} - \Delta H_{Exp}^{d}\right] + \Delta H_{Exp}^{d}}{\phi\left[\Delta H_{TNT}^{c} - \Delta H_{TNT}^{d}\right] + \Delta H_{TNT}^{d}} W_{Exp} \qquad \text{Eq. (2.5)}$$

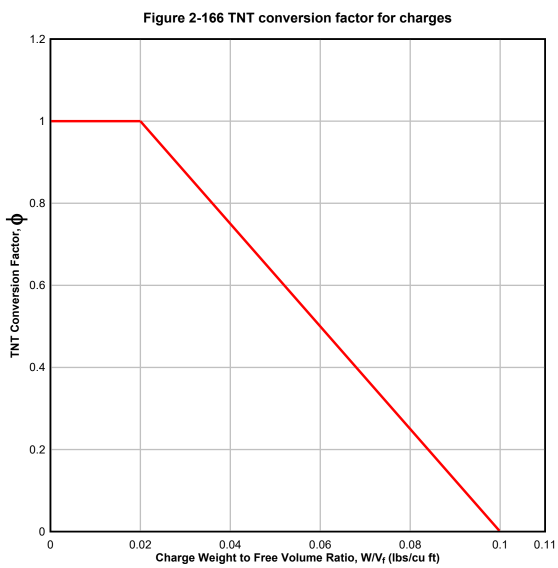

Figure 1 – TNT conversion factor.

When the charge-weight to free-volume ratio is beyond 0.1, the conversion factor, ϕ, is zero and the TNT-equivalence is a function of the heat-of-detonation ratio, implying that no afterburn is predicted for the given confinement volume. On the other extreme, for charge-weight to free-volume ratio less than 0.02, the TNT conversion factor, ϕ, is unity, implying that the TNT equivalence is only a function of the heat-of-combustion ratio and abundance of oxidizer is present.

$$W_{TNT} = \frac{\Delta H_{Exp}^{c}}{\Delta H_{TNT}^{c}} W_{Exp} \qquad \text{Eq. (2.6)}$$

2.3 LLNL Thermochemical Approach

LLNL has stated that SCE engineering primarily utilizes their in-house thermochemical equilibrium and kinetics code, CHEETAH, for TNT-equivalence solutions. The code solves thermodynamic equations to find, either complete or partial, chemical equilibrium between product species, thereby directly computing the heat-of-detonation. CHEETAH is much more sophisticated than a simplified theoretical thermodynamic equilibrium procedure, yet it employs a similar process. For example, one feature is that CHEETAH computes dozens and dozens of reaction product gases and their respective temperature-dependent specific heats in determining peak gas pressures. The simplified thermodynamic equilibrium procedure typically accounts for 3 or 4 reaction product gases including water vapor, which altogether might account for 99% of product gases.

LLNL utilizes the ratio of energy-of-detonation per unit volume, divided by the respective theoretical maximum densities;

$$W_{TNT} = \frac{\left(\dfrac{\Delta E^{d}_{Exp}}{\rho_{o(Exp)}}\right)}{\left(\dfrac{\Delta E^{d}_{TNT}}{\rho_{o(TNT)}}\right)} W_{Exp} \qquad \text{Eq. (2.7)}$$

Upon making the slight modification of normalizing the explosion energy (i.e., units of kJ per unit volume) to the HE density (i.e., grams per unit volume), the equation becomes;

$$W_{TNT} = \frac{\Delta E^{d}_{Exp}}{\Delta E^{d}_{TNT}} W_{Exp} \qquad \text{Eq. (2.8)}$$

Energy-of-detonation per unit volume divided by the HE density becomes the heat-of-detonation, and in effect, the LLNL format is equivalent to the UFC-3-340-02 as used by LANL. The major difference between LANL and LLNL methods is with CHEETAH's application of the lower-bound heat-of-detonation for TNT.

Table 1 shows the CHEETAH (Version 9) parameters including the TNT-equivalence that are derived for HMX and PBX-9501 (i.e., 95% HMX, 2.5% Estane and 2.5% BDNPAF). Basically, for example, the mechanical energy (i.e., impulse-driven condition) ratio of 5.7023 kJ/g for PBX-9501 to 4.3464 kJ/g for TNT, provides the TNT-equivalence of 1.312, as calculated by CHEETAH. As stated in Section 2.1, the heat-of-detonation for TNT used in the LANL calculations is 5.90 kJ/g, or 36% higher than calculated via CHEETAH.

Table 1 – CHEETAH Detonation Parameters

HE	Mw (g/mol)	$(\rho_o)_{Std}$ (g/cm^3)	(ΔH_f) (cal/g)	$(\Delta E_d)_{Total}$ (kJ/g)	$(\Delta E_d)_{Mech}$ (kJ/g)	$(\Delta E_d)_{Therm}$ (kJ/g)	(ΔH_c) (kJ/g)	$(TNT\text{-}Eq)_{Total}$	$(TNT\text{-}Eq)_{Mech}$	$(TNT\text{-}Eq)_{Combust}$
TNT	227.132	1.654	-66.504	-4.4621	-4.3464	-0.11567	14.529	1.000	1.000	1.000
HMX	296.156	1.905	60.527	-5.8677	-5.8677	0.00	8.852	1.315	1.350	0.609
PBX-9501	292.870	1.859	27.286	-5.7024	-5.7024	0.00	9.370	1.278	1.312	0.645

In order to understand all details of TNT-Equivalence and determine whether the LLNL approach is applicable, a set of simplified numerical hydrodynamic calculations with the Sandia National Laboratories code, CTH, are provided.

2.4 Dynamic Regime for Vessel Design

It is necessary to provide an important distinction to design of protective structures, such as confinement vessels, within the complete regime of dynamic loading; whether the design is based purely upon impulse-dominated loading or a pressure-dominated pulse. In other words, as described in UFC-3-340-02;

> *"A protective element subjected to high intensity shock pressures may be designed for the impulse rather than the pressure pulse, only if the duration of the applied pressure acting on the element is short in comparison to its response time. However, if the time to reach maximum displacement is equal to or less than three times the load duration, then a simplified pressure pulse representing the full pressure-time relationship should be used for these cases."*

Although protective elements subjected to high-explosive blast loading are generally designed to impulsive loads, it actually depends on the pulse duration and natural frequency of the structure (i.e., square-root of the ratio of structural stiffness to mass). In general, the response time is long compared to the pulse duration, but both the pulse duration and response time should be calculated for each case to determine the appropriate design criteria. i.e., impulse-dominated vs. simplified pressure-dominated pulse.

A single-degree-of-freedom (SDOF) model may be used to determine whether the blast loading event is predominantly within the impulse-dominated regime, mixed-mode regime, or pressure-dominated regime, as described by Baker et al. (1983). Figure 2 depicts the two different regimes of structural response to the SDOF loading function, impulsive and quasi-static, with the region in between being the mixed-mode. The ordinate is merely the ratio of dynamic-displacement to static-displacement. The abscissa represents the product of pulse-duration, T, and fundamental circular-frequency of the structure, ω, giving units of (rad-sec/sec).

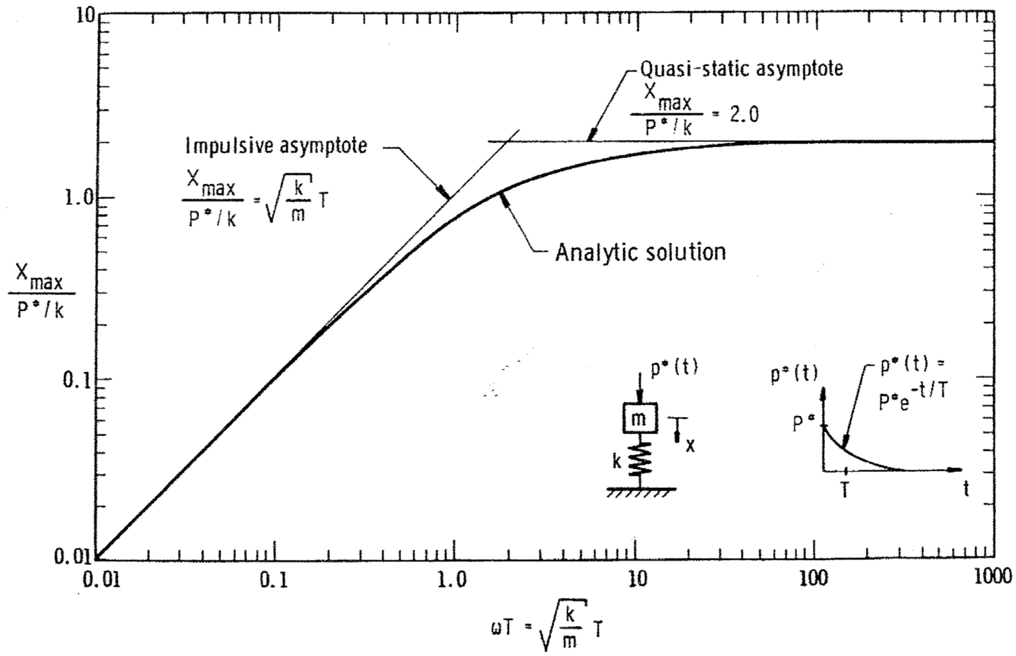

Figure 2 – SDOF structural response model for a pressure-pulse (Baker et al.).

Lastly, the ASME Boiler & Pressure Vessel Code, Sec. VIII, Div. 3 imposes requirements for design of impulsively loaded vessels, along with the following definition;

> *Impulsive loading is a loading whose duration is a fraction of the periods of the significant dynamic response modes of the vessel components. For a vessel, this fraction is limited to less than 35% of the fundamental, membrane-stress dominated (breathing) mode.*

The above statement implies that an impulsive event is defined as;

$$\frac{t_d}{T_s} \leq 0.35 \qquad \text{Eq. (2.9)}$$

where $t_d =$ Pressure pulse duration, (msec)

$T_s =$ Fundamental period of the structure, (msec)

To mitigate any confusion, please note that in Figure 2 the pulse-duration is T, but in the above equation pulse-duration is t_d and fundamental structural period is T_s. Therefore, a vessel design calculation must begin with determining whether the event is within the impulse-dominated or pressure-dominated regimes.

2.5 Code of Record and Standards Applicability

A 'Code of Record' as defined by DOE O 413.3B, *Program and Project Management for the Acquisition of Capital Assets*, is a set of design and operational requirements, including Federal and State laws, in effect at the time a facility or item of equipment was designed and accepted by DOE. The Code of Record for LANL application of HE Safety is DOE-STD-1212, *Explosives Safety*, which is implemented through LANL's HE Safety Program P101.8, *Explosives Safety*. It is important to note that these two safety programs reference TNT-equivalence as the common HE identifier when calculations are required or when an HE reference is identified. Therefore, it is important that this common method be adhered in calculations and documentation. Similarly, the Code of Record for vessel construction (Per 10 CFR § 851) is the 2015 version of the industry standard, ASME Boiler and Pressure Vessel Code, Section VIII, Division 3, *Alternatives Rules for the Construction of High-Pressure Vessels*, augmented with ASME Code Case 2564-4, *Impulsively Loaded Pressure Vessels Section VIII, Division 3*.

From DOE O 413.3B, PROGRAM AND PROJECT MANAGEMENT FOR THE ACQUISITION OF CAPITAL ASSETS

Code of Record.

A set of design and operational requirements, including Federal and state laws in effect at the time a facility or item of equipment was designed and accepted by DOE. It is (i) initiated during the conceptual design phase, placed under configuration control to ensure it is updated to include more detailed design requirements as they are developed during preliminary design, (ii) controlled during final design and construction with a process for reviewing and evaluating new and revised requirements to determine their impact on project safety, cost and schedule before a decision is taken to revise the Code of Record, and (iii) maintained and controlled through facility decommissioning. The Code of Record may be defined in contracts, Standards or Requirements Identification Documents (or their equivalent), or project-specific documents. [DOE-STD-1189-2016]

3.0 SHOCK LOADING

Computational models are developed for both PBX-9501 and TNT high-explosives (HE), and thus evaluate each in a consistent manner. The CTH models are 1D spherical geometry with the dimensions shown in Figure 3, that include the HE (i.e., TNT or PBX-9501 or HMX), Air at STP, and 2.5-in thick steel shell. Equation-of-state (EOS) employed in CTH for reaction product gases is the Jones-Wilkins-Lee (JWL) form, based on cylinder test experimental data derived from multiple sources. Appropriate HE-radii are applied for different weight TNT, PBX-9501 or HMX, based on their respective density, as listed in Appendix A.

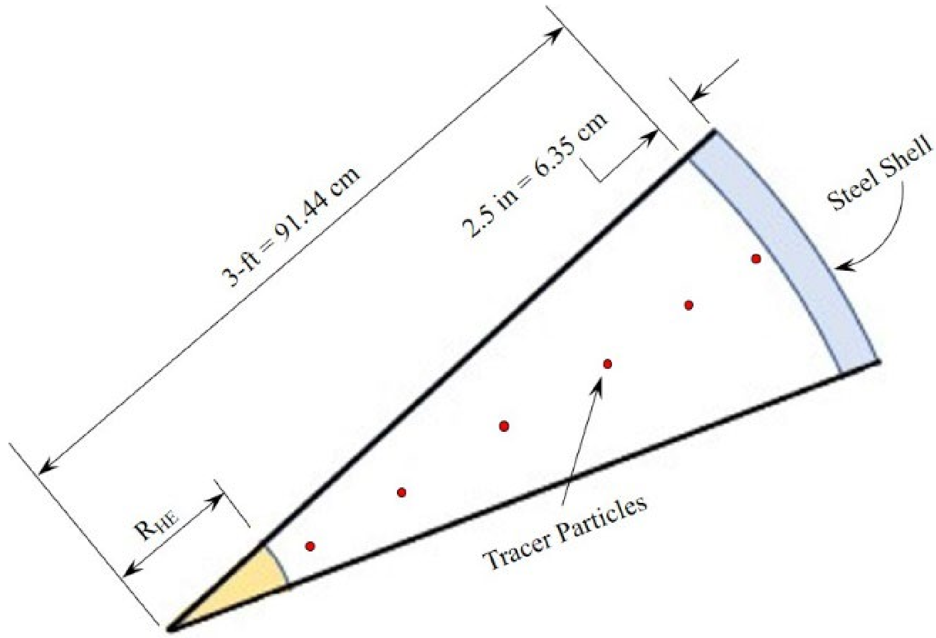

Figure 3 – 1D spherical CTH model

The amount of energy delivered by a HE detonation, within a constant-volume structure, such as a confinement vessel, is directly related to the heat-of-detonation, ΔH_d, of the specific explosive. As discussed in Section 2.1, the current methodology of equating the equivalent energy output of a mass of TNT to a different HE, is to determine the product of the mass of the new HE times the ratio the heats-of-detonation of the new explosive to that of TNT. Although this is the most widely used and accepted method, actual TNT-equivalence does not follow this process.

The mechanical energy delivered onto the structure is simply the overall internal surface integrated specific reflected impulse, or the area under the reflected pressure-time curve. Therefore, the intent herein is to determine the actual weight of a TNT charge that produces the same peak reflected impulse as would, say a 40-lb PBX-9501 charge, in a 6-ft ID vessel with no additional internal equipment. This concept was briefly discussed by King and Vaught relative to confined explosions in cylinders and spheres, where both peak pressure and impulse are important parameters depending on geometry. Also, recent work by Locking demonstrates the variation of TNT-equivalence as a function of positive phase impulse for explosions in free-air. Furthermore, Xiao et. al. demonstrated the difficulties with much of the current state of TNT-equivalence, and developed fitting coefficients to free-air burst blast data (i.e., peak side-on pressure and peak side-on impulse) as a function of scaled distance. The findings support the notion that at small scaled distances, the TNT-equivalence factor is non-uniform, while in the far-field range, equivalences appear invariant. Herein, however, through application of actual vessel geometries, TNT-equivalence factors are developed by comparing to the respective peak reflected specific impulse.

3.1 CTH Analyses

Two separate sets of CTH runs were conducted;

(1) high-fidelity cell-sizing to determine peak reflected pressures and impulse at shell wall for 3-ms span, and

(2) low-fidelity to determine the long-term quasi-static pressure after ~20-ms.

Noted below in Table 2 and Table 3, a listing of details of the HE-charge mass for PBX-9501 and TNT respectively and spherical dimensions for modeling in CTH. Each separate 1D spherical CTH analysis contains the HE-charge weight modeled as the exact HE radii for TNT or PBX-9501, along with the appropriate volume of air at standard temperature and pressure.

The closest tracer particle (see Figure 3), situated at 1.5 cell-widths away from the shell-wall, is monitored for peak reflected pressure and specific impulse. Cell sizing throughout was maintained at 0.05 cm/cell, except within the vicinity of the air-steel interface, which was refined to 0.01 cm/cell in order to achieve accurate representation of peak reflected pressures and impulses. A typical plot of the pressure-time history is shown below, namely a 40-lb bare spherical charge of PBX-9501. For all hydro runs, the peak reflected impulse (i_r) was chosen as the temporal region from the time-of-arrival (ToA) to the lowest pressure after the first pulse, as shown in Figure 6. This was consistently maintained to ensure adequate comparison, and thus each pressure plot for both PBX-9501 and TNT charge weight results were scanned to precisely determine the lowest pressure after the first pulse.

Results of computational effort are shown in Figure 7, comparing peak reflected impulse of TNT to PBX-9501. The first feature to notice is the linear relationship between HE-weight and peak reflected impulse, which is to be expected. The second feature to notice is a diverging trend between TNT and PBX-9501 as a function of HE-weight. This implies that for a peak reflected impulse using PBX-9501, the weight ratio of TNT to PBX-9501 results in successively higher values.

It is evident that if TNT-equivalence can be measured in terms of specific impulse, then Figure 7 shows that the actual TNT-equivalent factor is not a constant (i.e., a uniform single-valued number) throughout a range of explosive weights, but is actually variable. More importantly, what these calculations demonstrate is that the effective TNT-equivalent values are much lower than determined via CHEETAH.

Table 2 – Geometric Details for PBX-9501 charges

PBX-9501 CHARGE: CTH Results

ρ_o			
(g/cm^3)	(lb/in^3)		CHEETAH uses ρ_o = 1.859
1.859	0.0671606		CTH uses ρ_o = 1.84
			UCRL-52997 uses ρ_o = 1.855

Weight		HE Volume		HE Radius		Vessel Free Vol.	
(lb)	(g)	(in^3)	(cm^3)	(in)	(cm)	(in^3)	(cm^3)
10	4535.924	148.896744	2440.0	3.28800	8.35153	195283.3	3200119.92
15	6803.886	223.345116	3660.0	3.76382	9.56011	195208.9	3198899.929
20	9071.847	297.793488	4880.0	4.14262	10.52227	195134.4	3197679.939
25	11339.809	372.24186	6100.0	4.46251	11.33477	195060	3196459.949
30	13607.771	446.690232	7319.9	4.74212	12.04499	194985.5	3195239.959
35	15875.733	521.138604	8539.9	4.99216	12.68008	194911.1	3194019.968
40	18143.695	595.586976	9759.9	5.21938	13.25722	194836.6	3192799.978
45	20411.657	670.035348	10979.9	5.42837	13.78807	194762.2	3191579.988
50	22679.618	744.48372	12199.9	5.62241	14.28091	194687.7	3190359.998
55	24947.580	818.932092	13419.9	5.80390	14.74190	194613.3	3189140.008
60	27215.542	893.380464	14639.9	5.97470	15.17573	194538.8	3187920.017
65	29483.504	967.828836	15859.9	6.13625	15.58608	194464.4	3186700.027
70	31751.466	1042.277208	17079.9	6.28972	15.97590	194389.9	3185480.037
75	34019.428	1116.72558	18299.9	6.43605	16.34756	194315.5	3184260.047
80	36287.390	1191.173952	19519.8	6.57601	16.70305	194241	3183040.056
85	38555.351	1265.622324	20739.8	6.71025	17.04403	194166.6	3181820.066
90	40823.313	1340.070696	21959.8	6.83932	17.37188	194092.1	3180600.076
95	43091.275	1414.519068	23179.8	6.96370	17.68780	194017.7	3179380.086
100	45359.237	1488.96744	24399.8	7.08379	17.99282	193943.2	3178160.095

Table 3 – Geometric Details for TNT charges

TNT CHARGE: CTH Results

ρ_o			
(g/cm^3)	(lb/in^3)		CHEETAH uses ρ_o = 1.654
1.654	0.059755		CTH uses ρ_o = 1.630
			UCRL-52997 uses ρ_o = 1.654

HE Weight		HE Volume		HE Radius		Vessel Free Vol.	
(lb)	(g)	(in^3)	(cm^3)	(in)	(cm)	(in^3)	(cm^3)
10	4535.9	167.3513	2742.4	3.41859	8.68321	195264.8445	3199817.504
15	6803.9	251.0269	4113.6	3.91331	9.93980	195181.1688	3198446.305
20	9071.8	334.7026	5484.8	4.30715	10.94017	195097.4932	3197075.107
25	11339.8	418.3782	6856.0	4.63974	11.78494	195013.8175	3195703.909
30	13607.8	502.0539	8227.2	4.93046	12.52336	194930.1419	3194332.711
35	15875.7	585.7295	9598.4	5.19042	13.18368	194846.4663	3192961.513
40	18143.7	669.4052	10969.6	5.42667	13.78374	194762.7906	3191590.314
45	20411.7	753.0808	12340.8	5.64397	14.33567	194679.115	3190219.116
50	22679.6	836.7565	13712.0	5.84570	14.84809	194595.4393	3188847.918
55	24947.6	920.4321	15083.2	6.03440	15.32739	194511.7637	3187476.72
60	27215.5	1004.108	16454.4	6.21199	15.77845	194428.088	3186105.522
62	28122.7	1037.578	17002.9	6.28026	15.95185	194394.6177	3185557.042
65	29483.5	1087.783	17825.6	6.37996	16.20510	194344.4124	3184734.323
70	31751.5	1171.459	19196.8	6.53952	16.61039	194260.7367	3183363.125
75	34019.4	1255.135	20568.0	6.69166	16.99682	194177.0611	3181991.927
80	36287.4	1338.81	21939.2	6.83718	17.36643	194093.3854	3180620.729
85	38555.4	1422.486	23310.4	6.97675	17.72094	194009.7098	3179249.53
90	40823.3	1506.162	24681.6	7.11095	18.06181	193926.0341	3177878.332
95	43091.3	1589.837	26052.8	7.24027	18.39028	193842.3585	3176507.134
100	45359.2	1673.513	27424.0	7.36513	18.70742	193758.6828	3175135.936

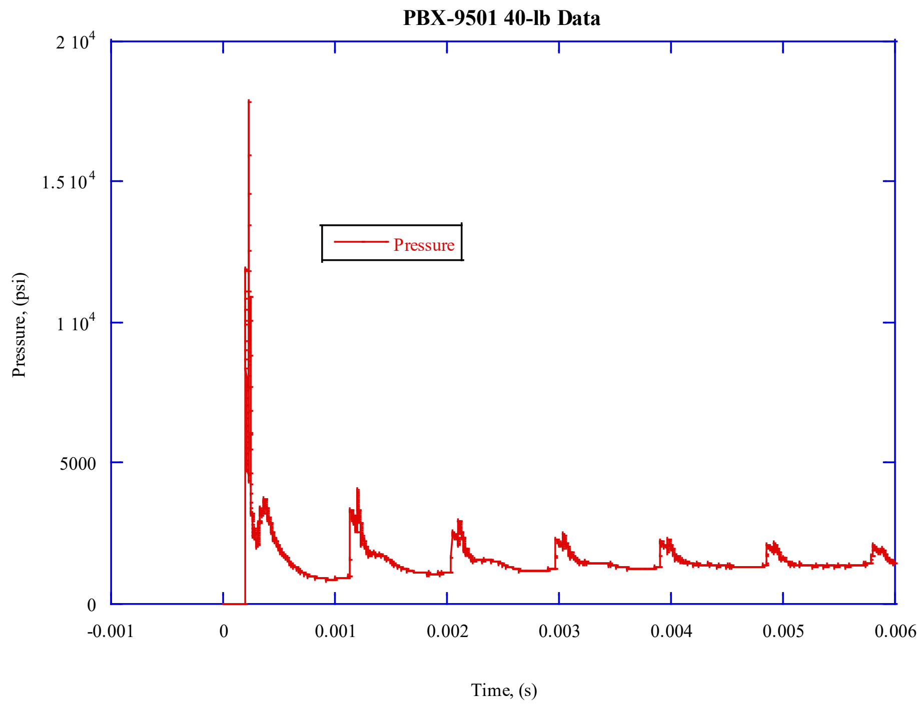

Figure 4 – Typical P-t history in 6-ft ID vessel.

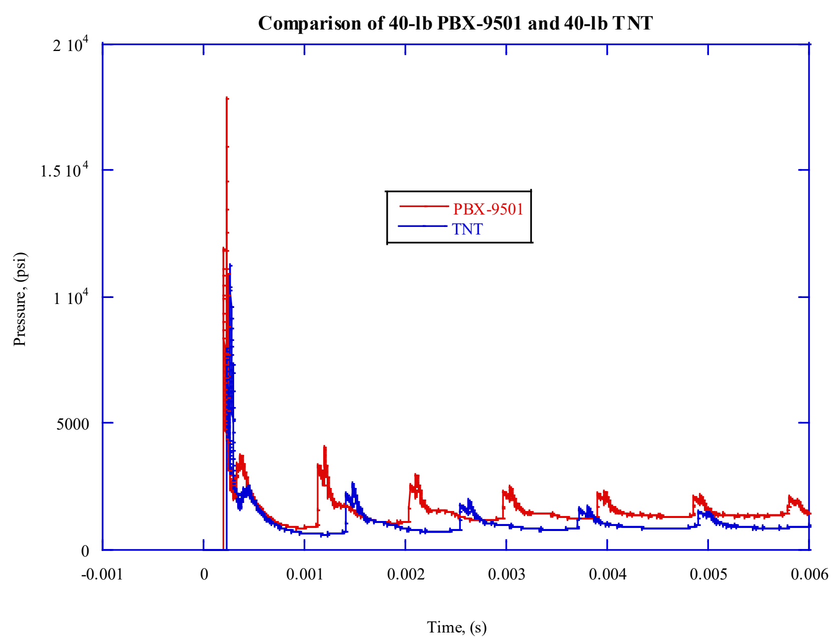

Figure 5 – Comparison of PBX-9501 and TNT for equal mass 40-lb charges.

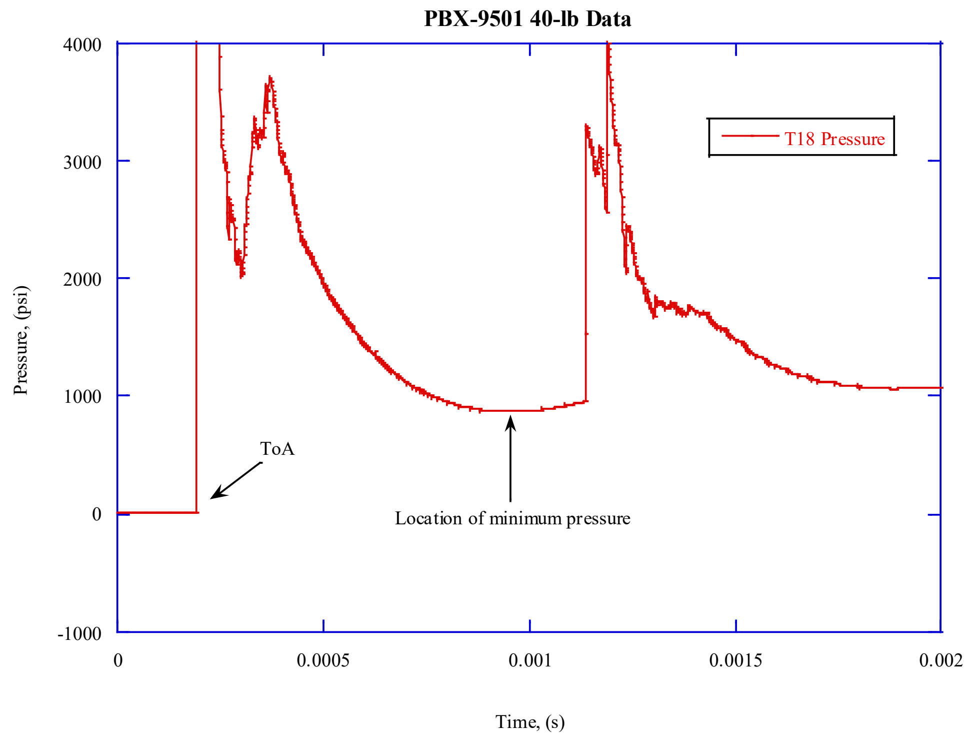

Figure 6 – Minimum pressure location after first pulse.

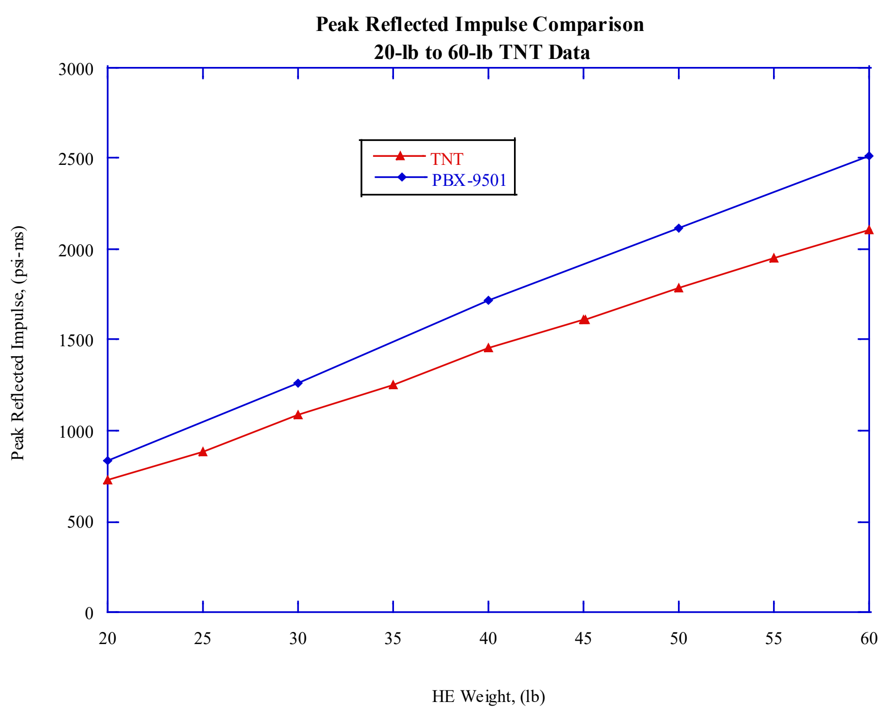

Figure 7 – Peak reflected impulse comparison with CTH JWL.

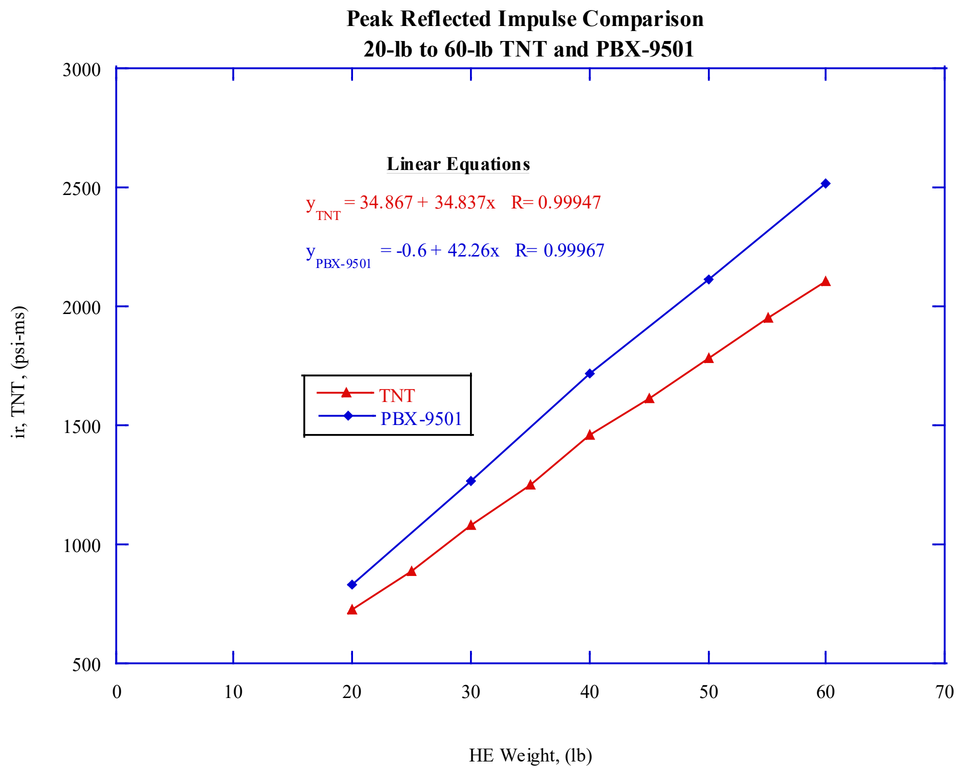

Figure 8 – Linearized equations for peak reflected impulse with CTH JWL.

Linear trends of Figure 7 and Figure 8 are represented by Eq. (3.1) and Eq. (3.2), where y represents the specific impulse:

$$y_{PBX} = 42.26x - 0.60 \quad \text{Eq. (3.1)}$$

$$y_{TNT} = 34.837x + 34.867 \quad \text{Eq. (3.2)}$$

Using the above linear equations to determine the equivalent weight of TNT for a given weight of PBX-9501, Table 4 presents results of Figure 7 and Figure 8 revealing that, in fact, there is a non-uniform TNT-equivalence and furthermore, it is not a constant single-value of 1.312 as presented in CHEETAH calculations (shown in Table 1).

Table 4 – TNT-Equivalence for Peak Reflected Impulse Using Reference JWL in CTH 1DS Model

PBX Weight (lb)	i_r, (psi-ms)	TNT Weight (lb)	TNT-Equivalence
10	422	11.11	1.111
20	845	23.25	1.163
30	1267	35.37	1.179
40	1690	47.51	1.188
50	2112	59.62	1.192
60	2535	71.77	1.196

Obviously, this exercise is only representative of a 6-ft ID empty vessel, minus the HE-ball volume. Other geometries would need to be investigated to determine whether the trends of Figure 7 are consistent and whether additional reaction products combustion has any effect. However, it is believed that for impulse conditions only (i.e., mechanical energy in CHEETAH terminology) the divergent linear trends will be consistent for other vessel geometries and structures, because full-combustion occurs subsequent to a detonation and only drives the peak gas pressure.

3.2 CHEETAH JWL Function

The CHEETAH derived JWL fit to both TNT and PBX-9501 were implemented into CTH as a User function. Similar 1D spherical analyses were conducted throughout the range of 20-lb to 60-lb, showing a P-t comparison, as depicted in Figure 9 between CTH JWL and CHEETAH JWL results for a 40-lb charge. Specific impulse results comparison of TNT and PBX-9501 are presented in Figure 10 using the CHEETAH derived JWL function, emphasizing a similar trend exhibiting the linearity between HE-weight and peak reflected impulse. Likewise, the divergent feature between TNT and PBX-9501 is indicative of their respective heats-of-detonation.

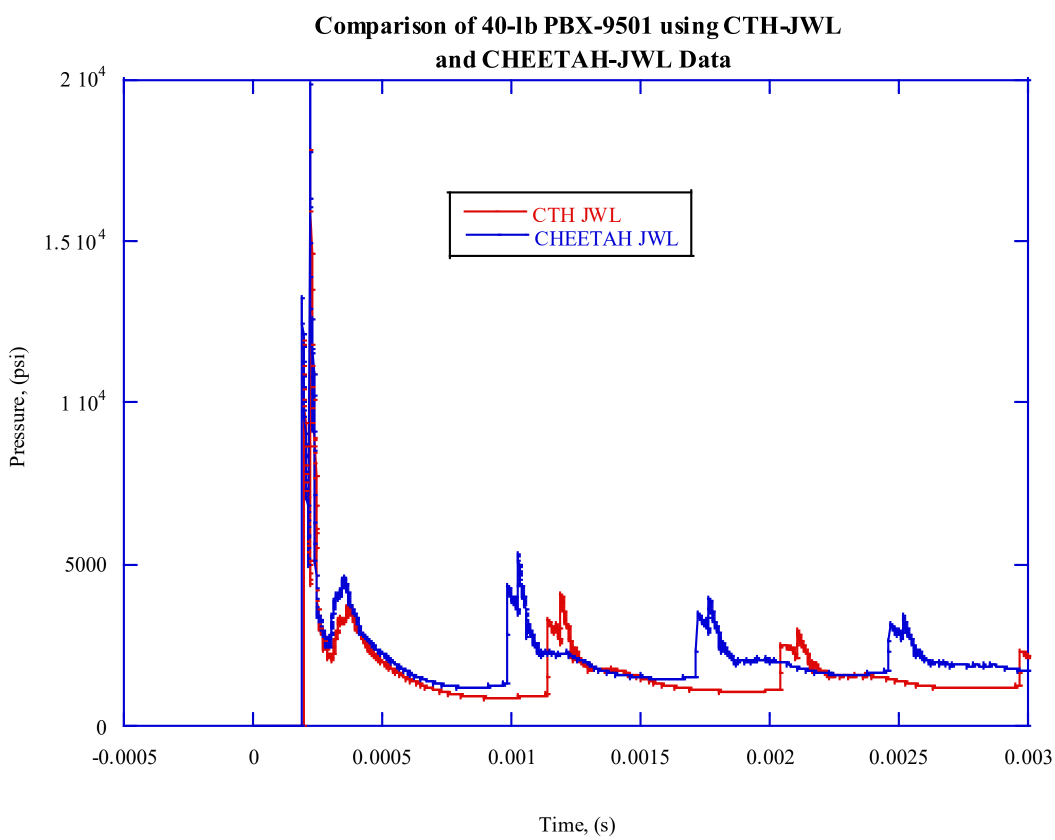

Figure 9 – Comparison of CTH JWL and CHEETAH JWL.

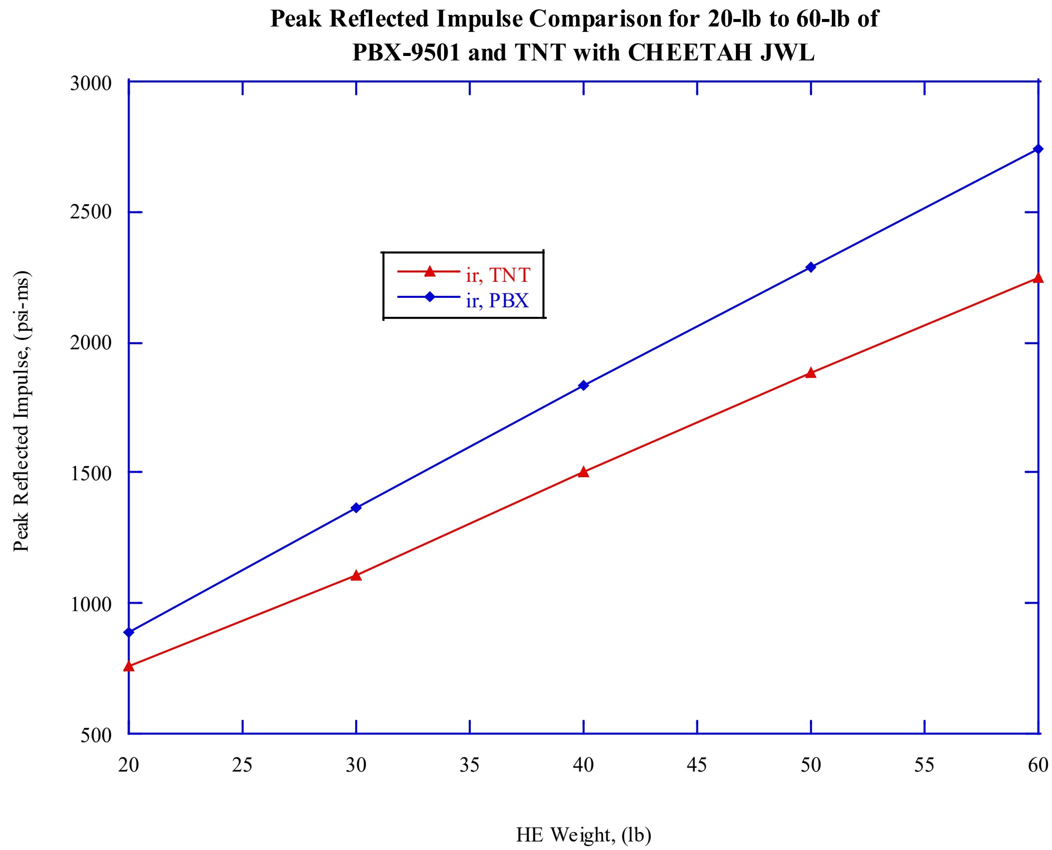

Figure 10 – Peak reflected impulse comparison with CHEETAH JWL.

Linear trends of Figure 10 and Figure 11 and are represented by Eq. (3.3) and Eq. (3.4):

$$y_{PBX} = 46.3x - 27 \quad \text{Eq. (3.3)}$$

$$y_{TNT} = 37.48x + 0.80 \quad \text{Eq. (3.4)}$$

Data from Figure 11 linear functions is listed in Table 5.

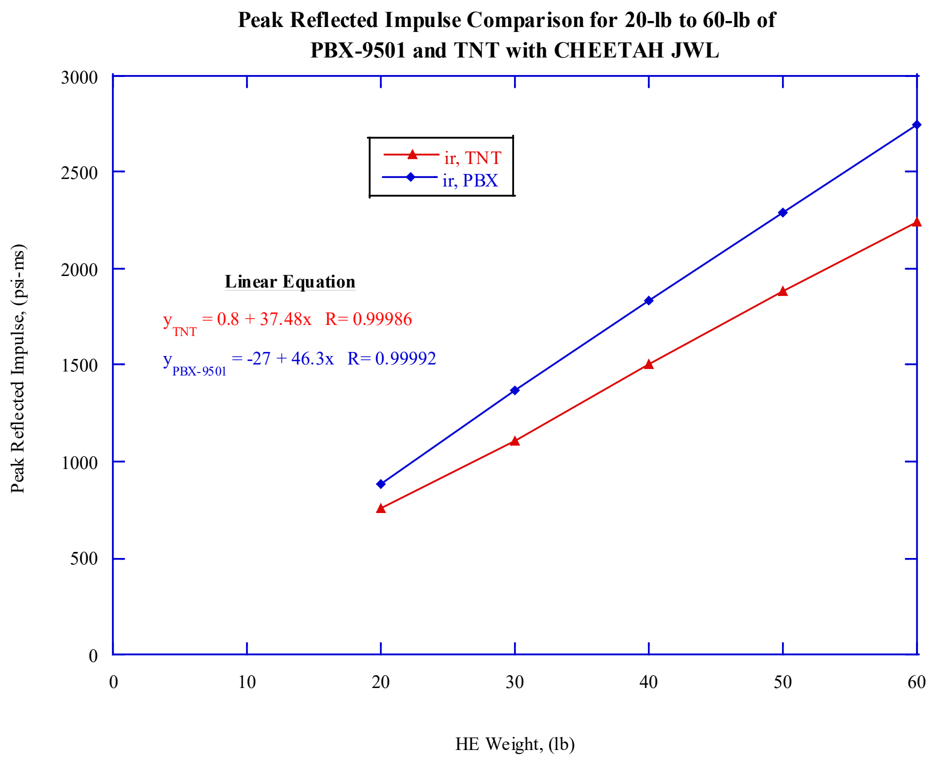

Figure 11 – Linearized equations for peak reflected impulse with CHEETAH JWL.

Table 5 – TNT-Equivalence for Peak Reflected Impulse Using CHEETAH JWL in CTH 1DS Model

PBX Weight (lb)	i_r, (psi-ms)	TNT Weight (lb)	TNT-Equivalence
10	436	11.61	1.161
20	899	23.96	1.198
30	1362	36.32	1.211
40	1825	48.67	1.217
50	2288	61.02	1.220
60	2751	73.38	1.223

Although the CTH reference JWL and the CHEETAH derived JWL parameters differ, in some instances by a significant amount, the results of Table 4 and Table 5 clearly show that the TNT-equivalence based on specific impulse are within a very narrow range for the 20-lb to 60-lb charge sizes. However, a value of 1.312, as computed by CHEETAH (see Table 1) is not evident in either Table 4 nor Table 5, and might possibly reach a value of 1.312 at much higher HE charge sizes. Figure 12 provides an overall comparison between the CTH JWL and CHEETAH derived JWL, showing differences that may be attributable to theoretical thermochemical construct (i.e., CHEETAH JWL) vs experimental data (CTH JWL).

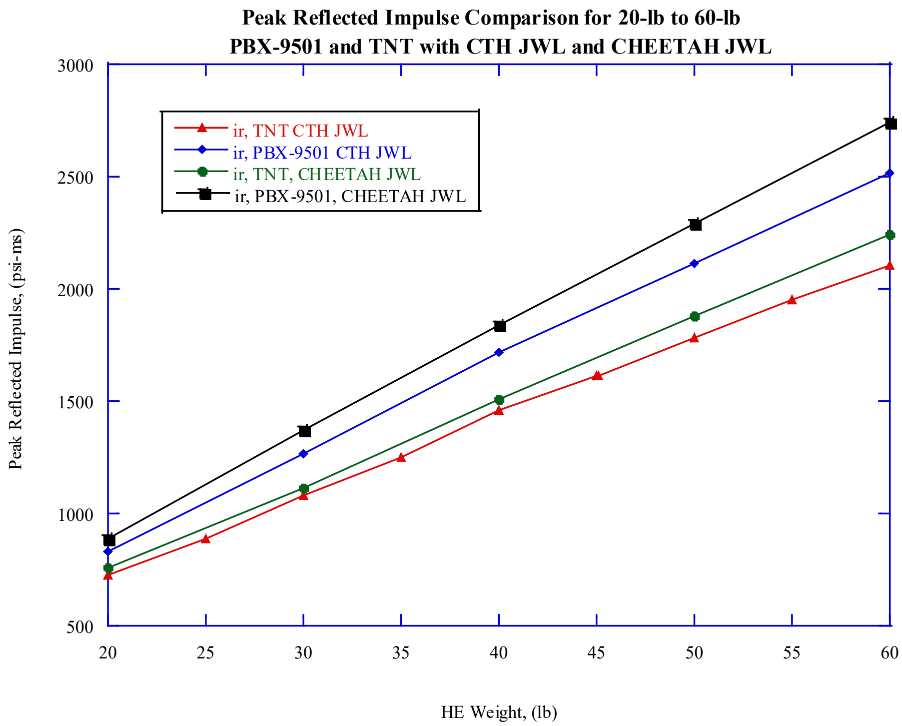

Figure 12 – Peak reflected impulse comparison with CTH and CHEETAH JWL.

It is evident by inspection of Figure 12 that either CTH reference JWL or the CHEETAH-derived JWL functions would provide similar (but not consistent) results in terms of peak reflected specific impulse, and by extension a similar TNT-equivalence.

4.0 PEAK EXPLOSION QUASI-STATIC GAS PRESSURE

Herein, two conditions are discussed; (1) confinement vessel gas pressure from detonation and partial secondary combustion (i.e., limited oxygen availability) and (2) U1a facility zero-room gas pressurization from an assumed vessel breach, where the zero-room atmosphere is assumed to have an abundance of oxidizer for a full-combustion afterburn.

4.1 Confinement Vessel Gas Pressure

The previous section dealt with the mechanical energy, i.e., a high-explosive detonation producing a specific impulse that drives the structural response of a structure. Here, the discussion focuses on peak quasi-static gas pressure, which has two components;

1. reaction products expansion from detonation event and
2. additional secondary (full or partial) combustion of reaction product gases with available oxidizer.

Thus, in determining the peak gas pressure, the 1D spherical model cell-sizing was maintained at 0.05 cm/cell throughout as the interest here is not in peak reflected pressures and impulse, but rather the long-term quasi-static pressure. In other words, we would like to determine the actual mass of TNT that results in a peak gas pressure equivalent to a specific mass of PBX-9501. Again, the concern is not with specific impulse, but rather the long-term quasi-static pressure. Thus, each numerical run was extended to 60-ms thus ensuring that no further pressure perturbations would affect the steady-state quasi-static pressure, long before heat-transfer effects are active.

It should be understood that the CTH-library JWL EOS function does not capture the effects of additional oxidizer, or oxygen deficient environments. As such, these results are purely based on the gas expansion due to a detonation only, no further combustion afterburn is considered in the analysis.

A typical plot of a pressure-time history is shown in Figure 13 to 6-ms time-frame, while Figure 14 and Figure 15 provide an extended view to 60-ms resulting in a steady-state behavior.

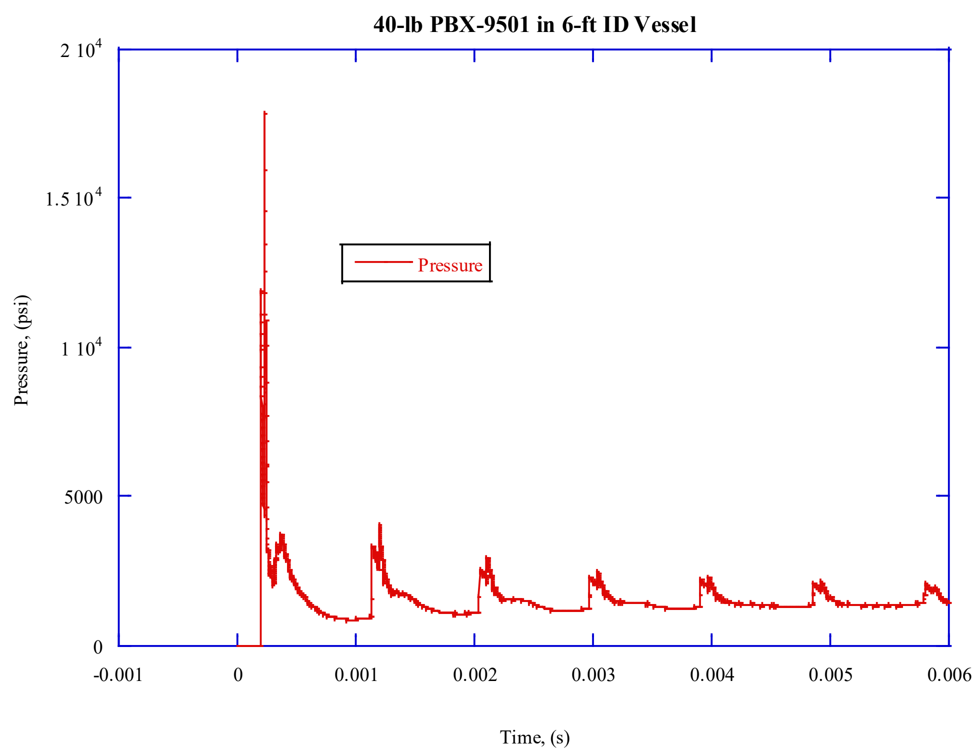

Figure 13 – Typical P-t history to 6-ms.

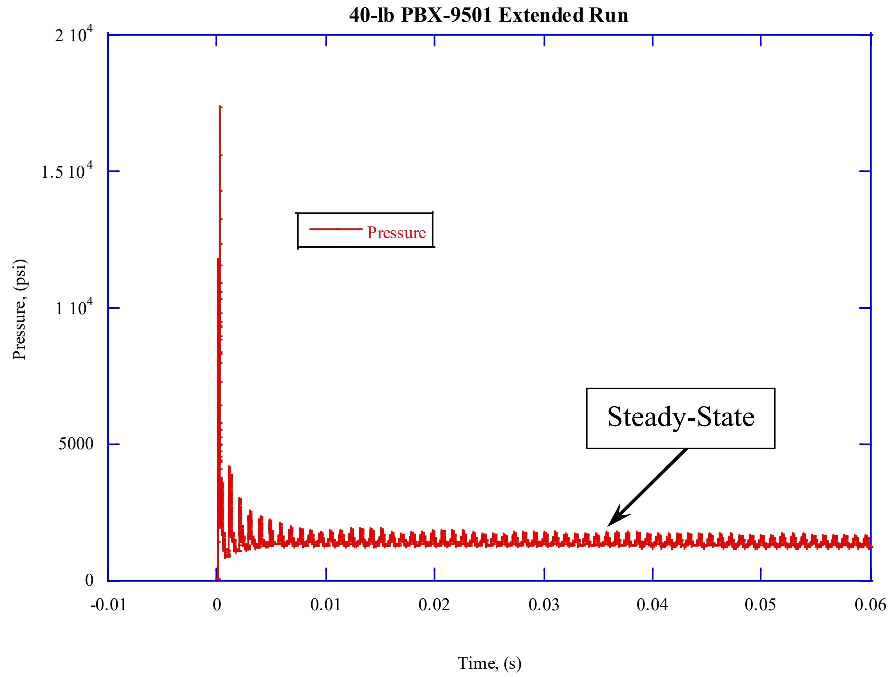

Figure 14 – Typical P-t history extended to 60 ms.

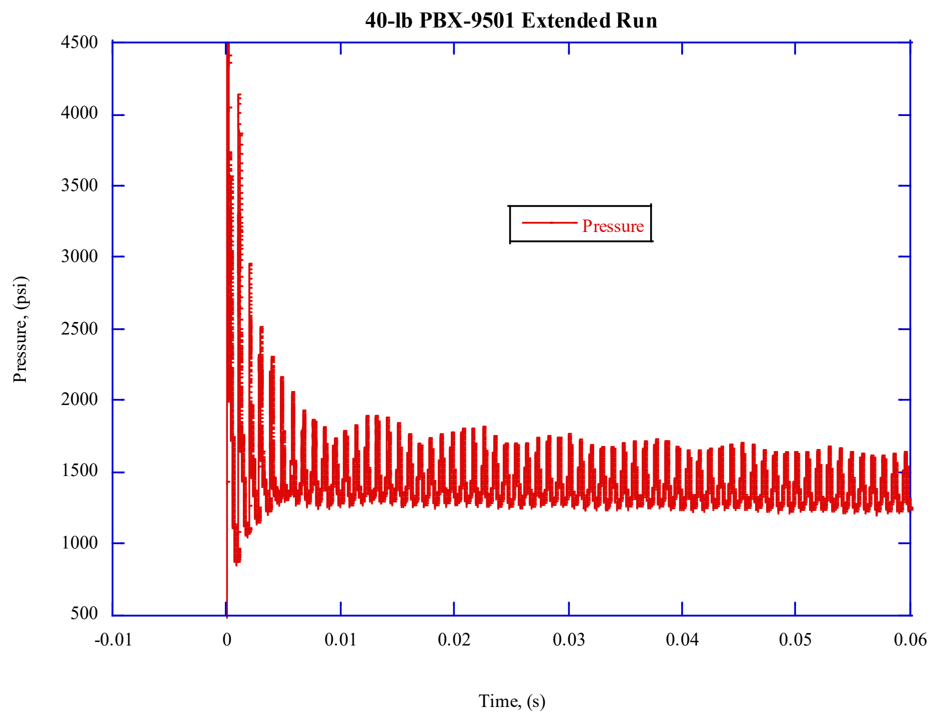

Figure 15 – Zoom view of P-t history extended to 60-ms.

In order to determine a consistent means of choosing the peak gas pressure for all numerical runs, an arbitrary value of 40-ms was chosen to select the pressure. No additional effort was made to extend the time-scale beyond the 60-ms limit, as this seemed reasonable.

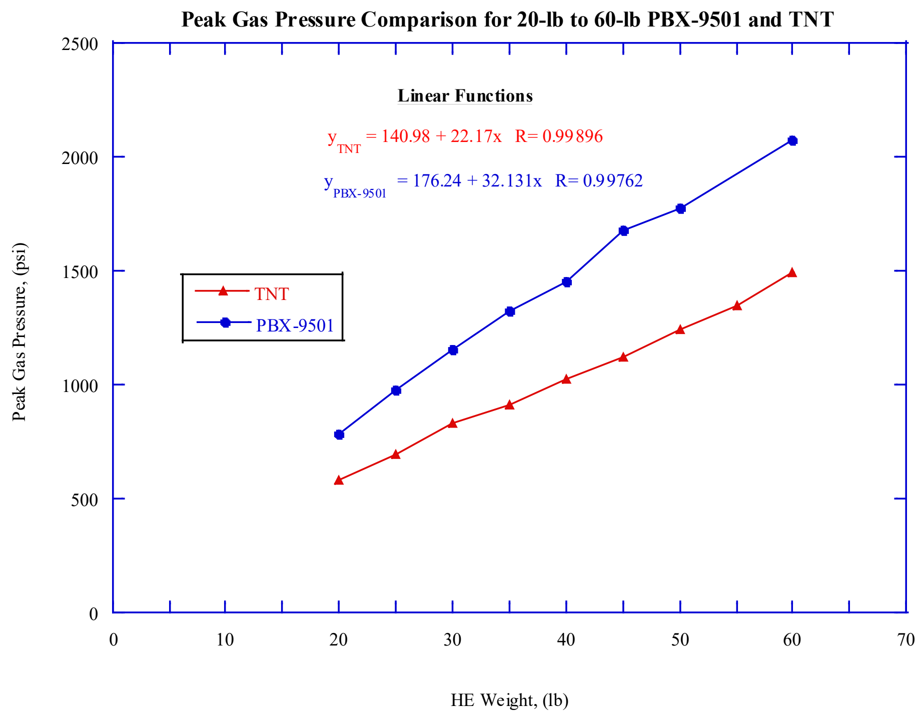

Figure 16 – Peak gas pressure comparison for PBX-9501 and TNT in vacuum.

Based on Figure 16, the peak gas pressures will result in TNT-equivalent factors as shown in Table 6, and it should be noted that each data point of Figure 16 is a separate CTH analysis.

$$y_{TNT} = 22.17x + 140.98 \quad \text{Eq. (4.1)}$$

$$y_{PBX-9501} = 32.131x + 176.24 \quad \text{Eq. (4.2)}$$

Table 6 – TNT-Equivalence of PBX-9501 Based on Peak Gas Pressure using CTH-JWL in Vacuum

PBX Weight (lb)	P_g, (psi)	TNT Weight (lb)	TNT-Equivalence
10	497.6	16.1	1.61
20	818.9	30.6	1.53
30	1140	45.1	1.50
40	1461	59.6	1.49
50	1783	74.1	1.48
60	2104	88.5	1.475

In comparing CHEETAH constant-volume explosion calculations between TNT and PBX-9501 under a vacuum environment, a similar divergent trend of peak gas pressure vs HE-weight is evident as shown in Figure 17, leading to a non-constant TNT-equivalent factor. The geometry used herein is a 6-ft ID vessel with no additional equipment/furniture, with the exception of reducing the free-volume by the volume occupied by the HE.

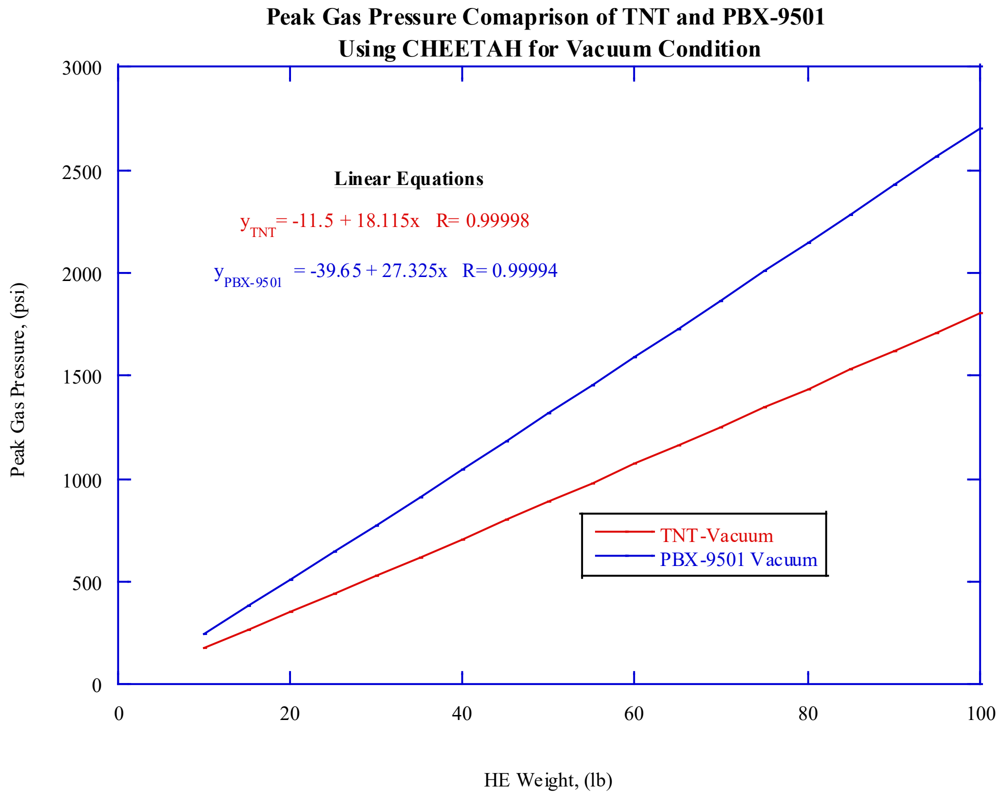

Figure 17 – CHEETAH comparison of peak gas pressure under vacuum for TNT and PBX-9501.

The above figure is based on a vacuum condition using CHEETAH constant-volume explosion models. Thus, Figure 17 can be compared directly with the CTH steady-state gas pressure results of Figure 16 and Table 6. Additionally, the effective TNT-equivalent factor for gas pressure appears to be a higher value than 1.312 as directly computed by CHEETAH (see Table 1). The linear equations of Figure 17 are represented by the following functions, and values listed in Table 7.

$$y_{TNT} = 18.115x - 11.5 \quad \text{Eq. (4.3)}$$

$$y_{PBX-9501} = 27.325x - 39.65 \quad \text{Eq. (4.4)}$$

Table 7 – TNT-Equivalence of PBX-9501 Based on Peak Gas Pressure in Vacuum Using CHEETAH

PBX Weight (lb)	P_g, (psi)	TNT Weight (lb)	TNT-Equivalence
10	233.6	13.53	1.353
20	506.9	28.61	1.431
30	780.1	43.70	1.457
40	1053.4	58.78	1.470
50	1326.6	73.87	1.477
60	1599.9	89.0	1.483

Figure 19 shows a comparison of peak gas pressure using CHEETAH, but accounting for available oxidizer in the vessel volume resulting in partial afterburn. Table 8 shows the TNT-equivalence of Figure 18 data, resulting in a TNT-equivalence of 1.45 for 40-lb PBX-9501.

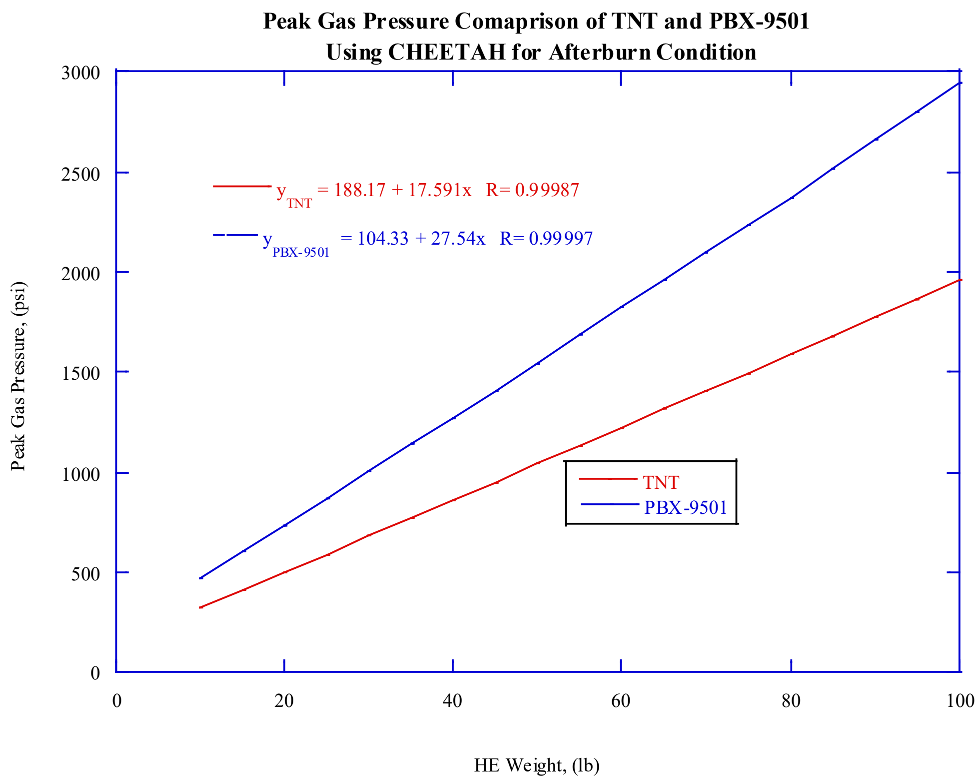

Figure 18 – CHEETAH comparison of peak gas pressure with afterburn for TNT and PBX-9501.

Table 8 – TNT-Equivalence of PBX-9501 Based on Peak Gas Pressure with Afterburn Using CHEETAH

PBX Weight (lb)	P_g, (psi)	TNT Weight (lb)	TNT-Equivalence
10	379.7	10.89	1.089
20	655.1	26.55	1.328
30	930.5	42.20	1.407
40	1205.9	57.86	1.447
50	1481.3	73.51	1.470
60	1756.7	89.17	1.486

Based purely on CHEETAH calculations and assuming no afterburn (i.e., vacuum), it appears that the effective peak gas pressure TNT-equivalent factor for PBX-9501, in a 6-ft ID air-filled vessel, ranges from 1.35 to 1.48 for HE-weights between 10-lb and 60-lb, respectively. For the partial afterburn case, TNT-equivalence factors range from 1.09 to 1.49 for PBX-9501 weights from 10-lb to 60-lb respectively. Again, this does not conform to the value of 1.312 directly provided from the thermochemical code CHEETAH, nor does it imply a uniform factor. Finally, Figure 19 shows the CTH steady-state gas pressure data compared with CHEETAH calculations for the vacuum case.

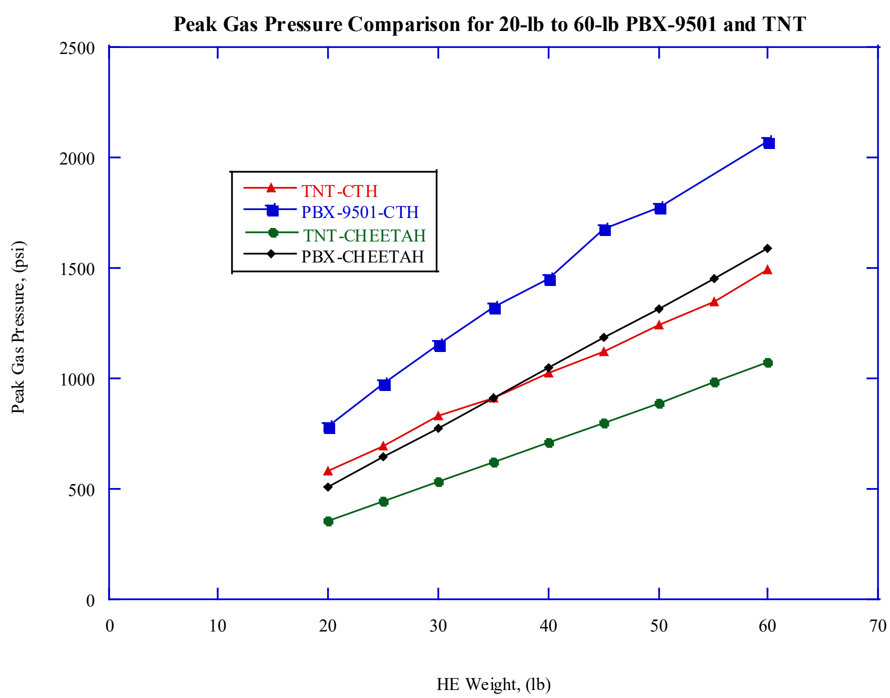

Figure 19 – Peak gas pressure for TNT and PBX-9501 with CTH 1D spherical and CHEETAH.

4.2 U1a Facility Zero-Rooms

Previously in Section 2.2, the LANL approach to utilizing TNT-equivalence was described, specifically referring to UFC-3-340-02. Herein, the guidance is extended to discuss oxygen rich environments at U1a facility.

Thus, UFC-3-340-02 provides a simple TNT-equivalence means for determining peak quasi-static gas pressures given a specified charge-weight to free-volume ratio, Eq. (4.5). In effect, this simple relationship accounts for the amount of oxidizer in the free-volume such that a null, partial or full-afterburn may be determined.

$$W_{TNT} = \frac{\phi\left[\Delta H^{c}_{Exp} - \Delta H^{d}_{Exp}\right] + \Delta H^{d}_{Exp}}{\phi\left[\Delta H^{c}_{TNT} - \Delta H^{d}_{TNT}\right] + \Delta H^{d}_{TNT}} W_{Exp} \qquad \text{Eq. (4.5)}$$

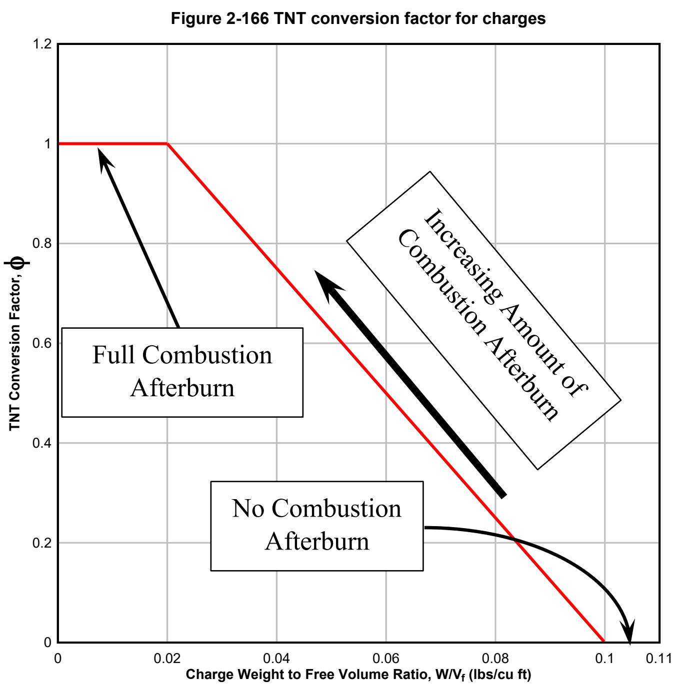

Figure 20 – TNT conversion factor.

When the charge-weight to free-volume ratio is beyond 0.1, the conversion factor, ϕ, is zero and the TNT-equivalence is only a function of the heat-of-detonation ratio, implying that no afterburn is predicted for the given confinement volume. On the other extreme, for charge-weight to free-volume ratio less than 0.02, the TNT conversion factor, ϕ, is unity, implying that the TNT equivalence is only a function of the heat-of-combustion ratio and abundant oxidizer is present.

$$W_{TNT} = \frac{\Delta H^{c}_{Exp}}{\Delta H^{c}_{TNT}} W_{Exp} \qquad \text{Eq. (4.6)}$$

Given a 40-lb PBX-9501 charge, the W/V ratio of 0.02 in Figure 20 corresponds to a free-volume of;

$$V = \frac{W}{0.02} \qquad \text{or} \qquad V = 2000 \text{ ft}^3$$

which is considered, for this case, the lower-bound volume for which a full-combustion afterburn is expected. Thus, for U1a facility zero-room volumes at, or above, 2000 ft^3, there is enough oxygen available for a full secondary combustion. Table 9 lists detonation and combustion properties for common SCE explosives used currently, or in the near future, at U1a facility zero-rooms. The TNT-equivalence for full-combustion is based on Eq. (4.6), using the heat-of-combustion, ΔH_c, ratio for the given explosive to that of TNT.

Table 9 – Detonation/Combustion Properties of SCE Explosives

HE	Density (g/cm^3)	Mol Weight (g/mol)	ΔH_d (kJ/g)	ΔH_c (kJ/g)	O_2 Balance % by Mass	TNT-Equiv (Full Combustion)	Composition
PBX-9501	1.8592	292.870	5.7024	9.3699	-26.875	0.645	95% HMX; 2.5% Estane; 2.5% BDNPA-F
LX-14	1.8537	289.373	5.6169	9.5931	-29.466	0.660	95.5% HMX; 4.5% Estane 5702-F1
HMX	1.905	296.156	5.8677	8.8519	-21.609	0.609	Pure HMX
TNT	1.654	227.132	4.3464	14.5290	-73.963	1.000	Pure TNT
TATB	1.937	258.149	4.1566	11.4318	-55.780	0.787	Pure TATB
PBX-9502	1.941	263.090	3.9909	11.1804	-54.926	0.770	95% TATB; 5% Kel-F 800
LX-17	1.943	265.6320	3.9019	11.0546	-54.498	0.761	92.5% TATB; 7.5% Kel-F 800

* Data taken from CHEETAH, Ver. 9

Based on the above combustion data of Table 9 and calculated TNT-equivalences, Table 10 lists the TNT-equivalent weight for three separate base-weights of explosives utilized in current and future SCE applications.

Table 10 – TNT-Equivalent Weight for Full Combustion with O_2 Rich Atmosphere

Base HE	Base HE Weight (lb)	TNT-Eq. Weight O_2 Rich - Full Combustion in U1a Facility (lb)	Composition
PBX-9501	40	26	95% HMX; 2.5% Estane; 2.5% BDNPA-F
	45	29	
	50	32	
PBX-9502	40	31	95% TATB; 5% Kel-F 800
	45	35	
	50	39	
LX-14	40	26	95.5% HMX; 4.5% Estane 5702-F1
	45	30	
	50	33	
LX-17	40	30	92.5% TATB; 7.5% Kel-F 800
	45	34	
	50	38	

5.0 COMPARISON OF JWL EOS AND HMX-BASED EXPLOSIVES

This section provides a comparison of CTH-derived JWL EOS for TNT, HMX, LX-14 and PBX-9501 with CHEETAH-derived JWL EOS parameters. Likewise, a comparison of detonation and combustion properties and parameters for HMX-based explosives only (HMX, LX-14 and PBX-9501) is provided that demonstrates a close resemblance in overall performance.

5.1 JWL EOS Comparison

The CTH code has an extended equation-of-state (EOS) library for high-explosive reaction products. The bulk of experimental data has been fit to the Jones-Wilkins-Lee (JWL) EOS, and derived from cylinder tests measuring the expansion and velocity of the metal cylinder wall. JWL parameters have been documented in many different sources, including Gibbs and Popolato, LLNL Explosives Handbook, and many other references. For TNT, HMX, LX-14 and PBX-9501, please note that Table 11 through Table 14 provide the library functions embedded in CTH, while Table 15 through Table 18 contain the CHEETAH derived data. Note that actual JWL format in CTH and CHEETAH differ slightly, including the units for JWL coefficients.

JWL form in CTH

$$P(\rho,T) = A\exp\left(-R_1\frac{\rho_o}{\rho}\right) + B\exp\left(-R_2\frac{\rho_o}{\rho}\right) + \omega\rho C_V T$$

JWL form in CHEETAH

$$P = A\exp\left[-R_1\frac{v}{v_o}\right] + B\exp\left[-R_2\frac{v}{v_o}\right] + C\left(\frac{v}{v_o}\right)^{-(1+\omega)}$$

Table 11 – JWL Parameters for TNT in CTH

CTH JWL PARAMETERS - TNT

ρ_o	T_o		v_o	AG	BG	R1	R2	WG	CV	T_{C-J}		E_o	D_{C-J}	P_{C-J}	
(g/cm^3)	(eV)	(K)	(cm^3/g)	(dyn/cm^2)	(dyn/cm^2)				(erg/g/eV)	(eV)	(K)	(dyn/cm^2)	(cm/s)	(dyn/cm^2)	(GPa)
1.63	0.02568	298.00	0.6134969	3.71E+12	3.23E+10	4.15	0.95	0.3	6.724E+10	0.350	4062	7.01E+10	6.93E+05	2.10E+11	21.01

Note: WG is ω

Unit Conversions					
1	eV	1	GPa	1	erg
11604.53	K	1.00E+10	dyn/cm^2	1	dyn-cm

Table 12 – JWL Parameters for HMX in CTH

CTH JWL PARAMETERS - HMX

ρ_o	T_o		v_o	AG	BG	R1	R2	WG	CV	$T_{C\text{-}J}$		E_o	$D_{C\text{-}J}$	$P_{C\text{-}J}$	
(g/cm^3)	(eV)	(K)	(cm^3/g)	(dyn/cm^2)	(dyn/cm^2)				(erg/g/eV)	(eV)	(K)	(dyn/cm^2)	(km/s)	(dyn/cm^2)	(GPa)
1.891	0.02568	298.00	0.52882073	7.78E+12	7.07E+10	4.20	1.00	0.30	9.909E+10	0.350	4062	1.29E+11	9.110	4.15E+11	41.50

Unit Conversions					
1	eV	1	GPa	1	erg
11604.525	K	1.00E+10	dyn/cm^2	1	dyn-cm

Note: WG is ω

Table 13 – JWL Parameters for LX-14 in CTH

CTH JWL PARAMETERS - LX-14

ρ_o	T_o		v_o	AG	BG	R1	R2	WG	CV	$T_{C\text{-}J}$		E_o	$D_{C\text{-}J}$	$P_{C\text{-}J}$	
(g/cm^3)	(eV)	(K)	(cm^3/g)	(dyn/cm^2)	(dyn/cm^2)				(erg/g/eV)	(eV)	(K)	(dyn/cm^2)	(cm/s)	(dyn/cm^2)	(GPa)
1.835	0.0256798	298.00	0.544959	8.261E+12	1.724E+11	4.55	1.32	0.38	5.527E+10	0.350	4062	1.02E+11	8.80E+05	3.700E+11	37.00

Unit Conversions					
1	eV	1	GPa	1	erg
11604.53	K	1.00E+10	dyn/cm^2	1	dyn-cm

Note: WG is ω

Table 14 – JWL Parameters for PBX-9501 in CTH

CTH JWL PARAMETERS - PBX-9501

ρ_o	T_o		v_o	AG	BG	R1	R2	WG	CV	$T_{C\text{-}J}$		E_o	$D_{C\text{-}J}$	$P_{C\text{-}J}$	
(g/cm^3)	(eV)	(K)	(cm^3/g)	(dyn/cm^2)	(dyn/cm^2)				(erg/g/eV)	(eV)	(K)	(dyn/cm^2)	(cm/s)	(dyn/cm^2)	(GPa)
1.84	0.0256798	298.00	0.5434783	8.52E+12	1.80E+11	4.6	1.3	0.38	5.527E+10	0.350	4062	1.02E+11	8.80E+05	3.70E+11	37.00

Unit Conversions					
1	eV	1	GPa	1	erg
11604.53	K	1.00E+10	dyn/cm^2	1	dyn-cm

Note: WG is ω

CHEETAH develops the JWL functions internally from the thermochemical and thermodynamic conditions of the explosive. As alluded to earlier, the functional form in CHEETAH is slightly different than that in CTH, yet has the same characteristics as the CTH functions. However, the individual parameters in some instances vary greatly, as evident from comparison of Table 11 through Table 14 with Table 15 through Table 18 below.

Table 15 – JWL Parameters for TNT in CHEETAH

CHEETAH JWL PARAMETERS - TNT

ρ_o	T_o		v_o	A	B	C	R1	R2	ω	$T_{C\text{-}J}$		E_o	$D_{C\text{-}J}$	$P_{C\text{-}J}$	
(g/cm^3)	(eV)	(K)	(cm^3/g)	(GPa)	(GPa)	(GPa)				(eV)	(K)	(kJ/cm^3)	(km/s)	(dyn/cm^2)	(GPa)
1.654	0.02568	298.00	0.6045949	1594.00	50.80	1.536	6.732	2.302	0.38778	0.350	4062	-7.189	7.20971	2.15E+11	21.49
				(dyn/cm^2)	(dyn/cm^2)	(dyn/cm^2)									
				1.594E+13	5.08E+11	1.54E+10									

Table 16 – JWL Parameters for HMX in CHEETAH

CHEETAH JWL PARAMETERS - HMX															
ρ_o	T_o		v_o	A	B	C	R1	R2	ω	T_{C-J}		E_o	D_{C-J}	P_{C-J}	
(g/cm^3)	(eV)	(K)	(cm^3/g)	(GPa)	(GPa)	(GPa)				(eV)	(K)	(kJ/cm^3)	(km/s)	(dyn/cm^2)	(GPa)
1.905	0.02568	298.00	0.52493438	4437.00	122.60	2.548	7.543	2.364	0.56	0.350	4062	-11.18	9.11886	3.96E+11	39.6019057
				(dyn/cm^2)	(dyn/cm^2)	(dyn/cm^2)									
				4.437E+13	1.226E+12	2.548E+10									

Table 17 – JWL Parameters for LX-14 in CHEETAH

CHEETAH JWL PARAMETERS - LX-14															
ρ_o	T_o		v_o	A	B	C	R1	R2	ω	T_{C-J}		E_o	D_{C-J}	P_{C-J}	
(g/cm^3)	(eV)	(K)	(cm^3/g)	(GPa)	(GPa)	(GPa)				(eV)	(K)	(kJ/cm^3)	(km/s)	(dyn/cm^2)	(GPa)
1.85375	0.0256798	298.00	0.539447	3281.00	110.30	2.251	7.268	2.36	0.51701	0.350	4062	-10.41	8.85201	3.485E+11	34.853
				(dyn/cm2)	(dyn/cm2)	(dyn/cm2)									
				3.2810E+13	1.1030E+12	2.2510E+10									

Table 18 – JWL Parameters for PBX-9501 in CHEETAH

CHEETAH JWL PARAMETERS - PBX-9501															
ρ_o	T_o		v_o	A	B	C	R1	R2	ω	T_{C-J}		E_o	D_{C-J}	P_{C-J}	
(g/cm^3)	(eV)	(K)	(cm^3/g)	(GPa)	(GPa)	(GPa)				(eV)	(K)	(kJ/cm^3)	(km/s)	(dyn/cm^2)	(GPa)
1.8592	0.0256798	298.00	0.5378657	3570.00	112.20	2.352	7.377	2.356	0.5308	0.350	4062	-10.60	8.90935	3.69E+11	36.89
				(dyn/cm^2)	(dyn/cm^2)	(dyn/cm^2)									
				3.57E+13	1.122E+12	2.35E+10									

Figure 21 and Figure 22 depict the CTH and CHEETAH JWL EOS for PBX-9501 and TNT. There are clear and obvious differences between the two EOS pairs, although within the region of interest, i.e., between relative specific volumes of 1.0 to 0.75 for PBX-9501 and TNT, the differences are not negligible, but workable.

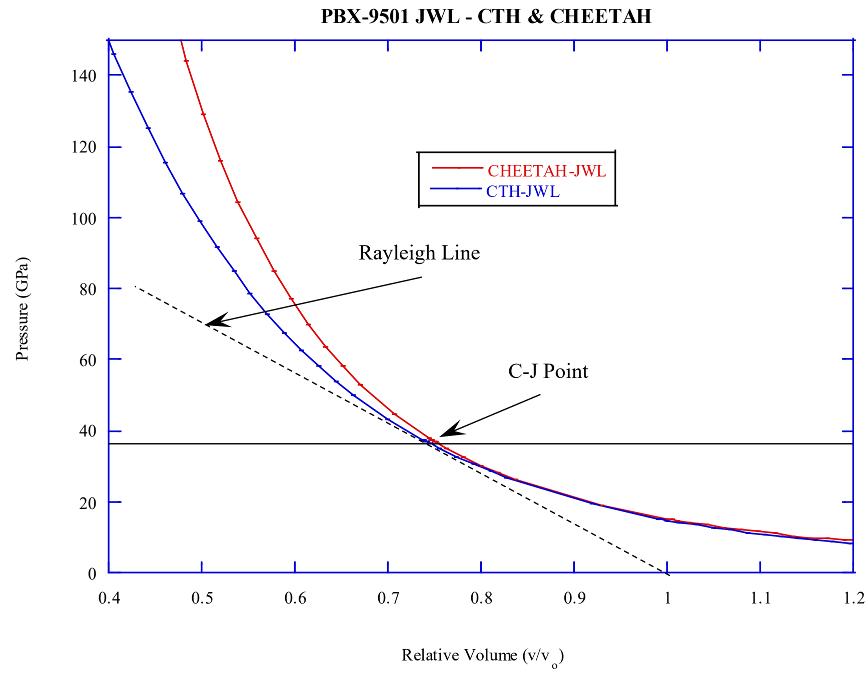

Figure 21 – PBX-9501 JWL EOS from CTH and CHEETAH

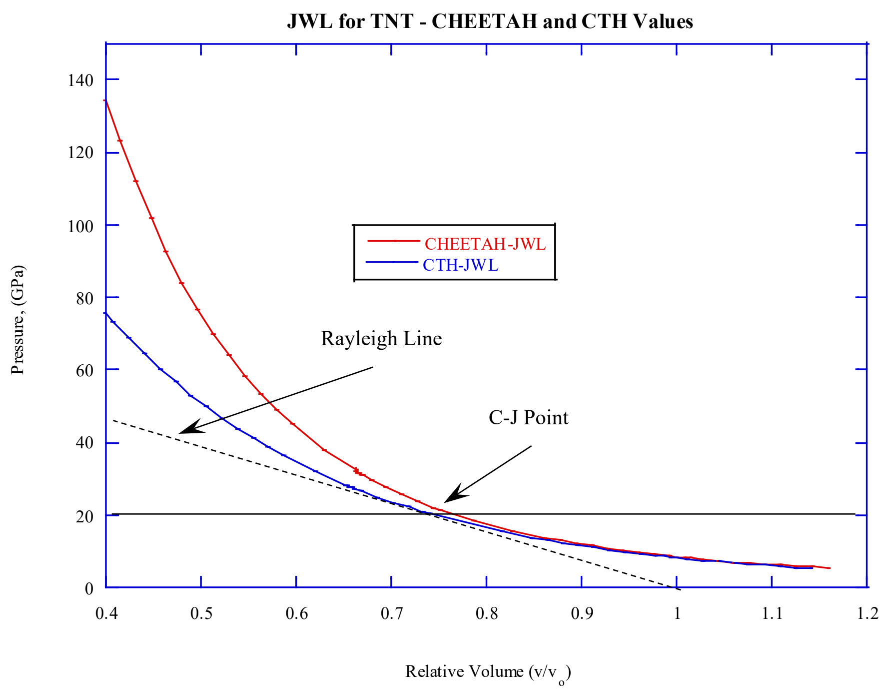

Figure 22 – TNT JWL EOS from CTH and CHEETAH

However, in order to determine whether there are significant issues with either code, the JWL EOS developed within CHEETAH is implemented herein as a USER function in subsequent CTH analyses for comparison, applying the 1D spherical model. Figure 23 and Figure 24 demonstrate the differences in the pressure-time history for a 40-lb PBX-9501 charge and 40-lb TNT charge, respectively, using the JWL EOS from CTH and CHEETAH. There are many obvious differences, such as peak reflected pressure, specific impulse and phasing of late-time reflections. To a lesser degree, in both the PBX-9501 and TNT curves, the peak pressure ToA between the CTH and CHEETAH curves are within 3μs. Nonetheless, it is evident there is slightly more energy in the P-t curve with the CHEETAH JWL formulation.

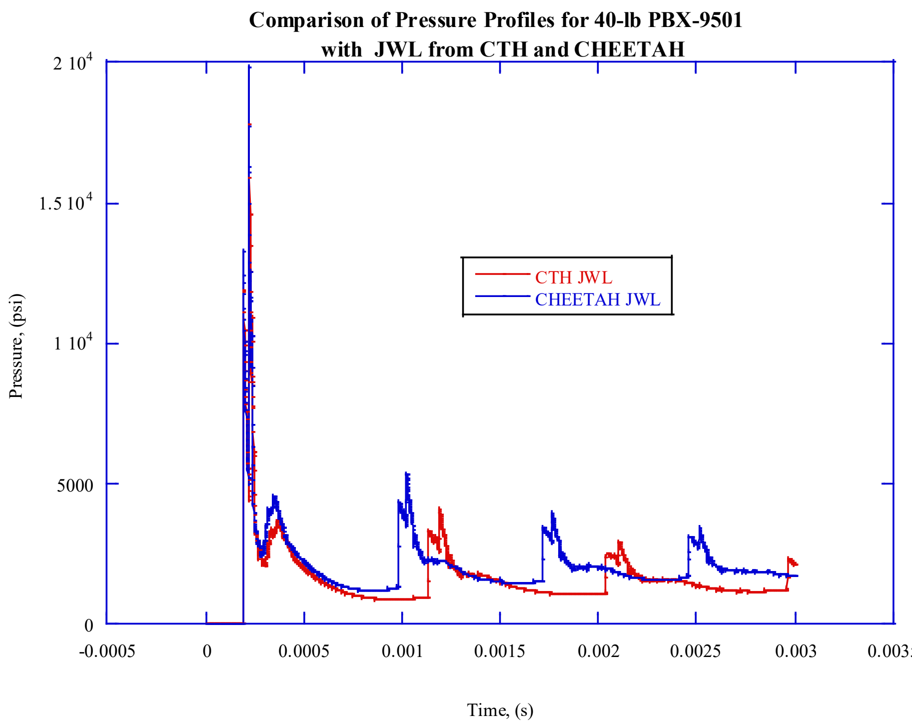

Figure 23 – Comparison of CTH JWL and CHEETAH JWL EOS for PBX-9501

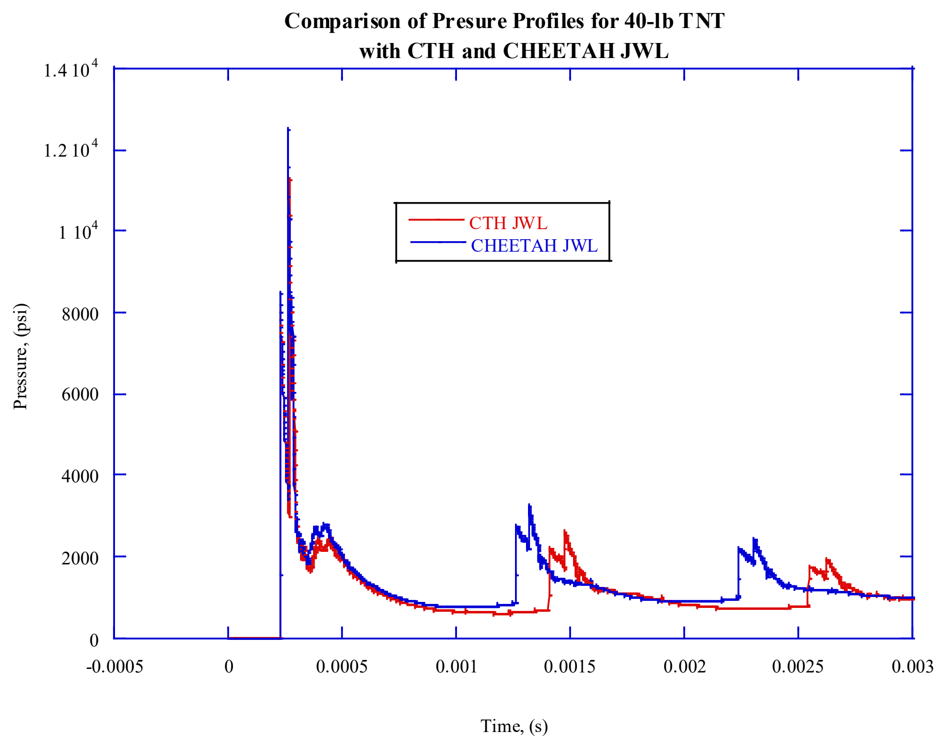

Figure 24 – Comparison of CTH and CHEETAH JWL EOS for TNT.

5.2 HMX-Based Explosives Comparison

A comparison of detonation and combustion parameters for HMX, LX-14 and PBX-9501 is provided herein to demonstrate that performance of all three explosives is consistent with minor variability. LX-14 is 95.5% HMX and 4.5% Estane 5702-F1, while PBX-9501 is 95% HMX, 2.5% Estane and 2.5% BDNPA-F. Thus, it would seem logical that both LX-14 and PBX-9501 would have similar detonation properties. The major difference between CTH-library data (Table 19) and CHEETAH (Table 20) is the density of LX-14 (i.e., 1.835 vs 1.85375 g/cm^3), while differences between other parameters are slight.

Table 19 – Data Derived from CTH Library

HE	Composition	Density (g/cm^3)	Mw (g/mol)	ΔH_f (kJ/g)	ΔH_d (kJ/g)	ΔH_c (kJ/g)	$P_{C\text{-}J}$ (GPa)	$D_{C\text{-}J}$ (km/s)
TNT	100% TNT	1.63	227.1	0.284	4.56	14.98	21.01	6.93
HMX	100% HMX	1.905	296.2	0.253	6.78	9.43	41.50	9.11
LX-14	95.5% HMX 4.5% Estane	1.835	289.4	0.0628	6.59	9.593*	37.00	8.80
PBX-9501	95% HMX 2.5% Estane 2.5% BDNPA-F	1.84	292.9	0.0954	6.65	9.40	37.00	8.80
						*Cheetah		

Table 20 – Data Derived from CHEETAH

HE	Composition	Density (g/cm^3)	Mw (g/mol)	ΔH_f (kJ/g)	ΔH_d (kJ/g)	ΔH_c (kJ/g)	P_{C-J} (GPa)	D_{C-J} (km/s)
TNT	100% TNT	1.654	227.132	0.2783	4.3464	14.53	21.49	7.21
HMX	100% HMX	1.905	296.156	0.2532	5.8677	8.852	39.6	9.19
LX-14	95.5% HMX 4.5% Estane	1.85375	289.373	0.0632	5.6169	9.593	34.853	8.85
PBX-9501	95% HMX 2.5% Estane 2.5% BDNPA-F	1.8592	292.87	0.1142	5.7022	9.37	36.89	8.91

Two separate evaluations are performed for each high-explosive formulation, using a 1DS CTH model of a 40-lb spherical HE-charge in a 6-ft ID vessel under vacuum conditions only;

(a) CTH-library HE parameters and EOS functions and

(b) CHEETAH-derived HE parameters and EOS functions.

Because the CTH JWL EOS cannot determine either partial or full afterburn, the CHEETAH analyses likewise were conducted under vacuum conditions thus having a direct comparison of detonation performance.

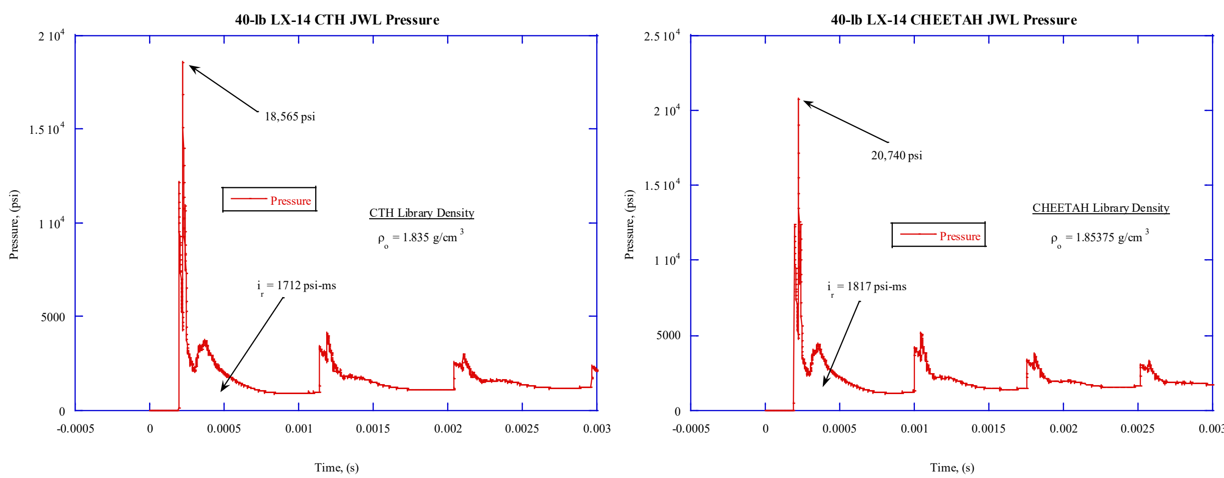

Figure 25 – Comparison of LX-14 performance with CTH and CHEETAH JWL EOS.

Comparison of above results show that, aside from the slightly higher HE-density, the CHEETAH-derived EOS properties run hotter than the CTH library EOS functions, resulting in slightly higher peak reflected pressure and peak reflected specific impulse.

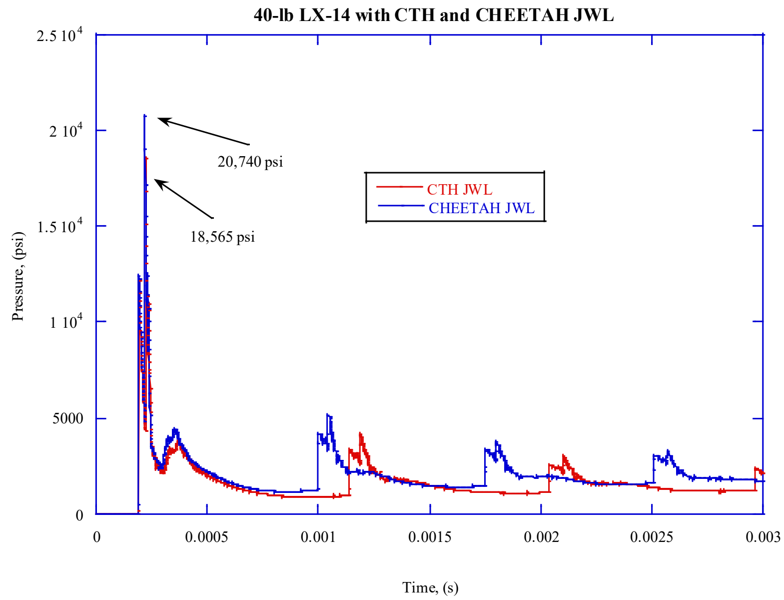

Figure 26 – LX-14 results comparison with CTH JWL and CHEETAH JWL.

Now, comparing all three HMX-based explosives under pure vacuum detonation, Figure 27 depicts the very slight variations. The right-hand side figure is displaced in time by 0.5 ms for LX-14 and PBX-9501 showing similarities. As evident from results listed in Table 21 for detonation pressures, all three explosives, HMX, LX-14 and PBX-9501, show similar peak reflected pressures but more importantly similar peak reflected specific impulse, which is the driving energy supplied to the confinement vessel.

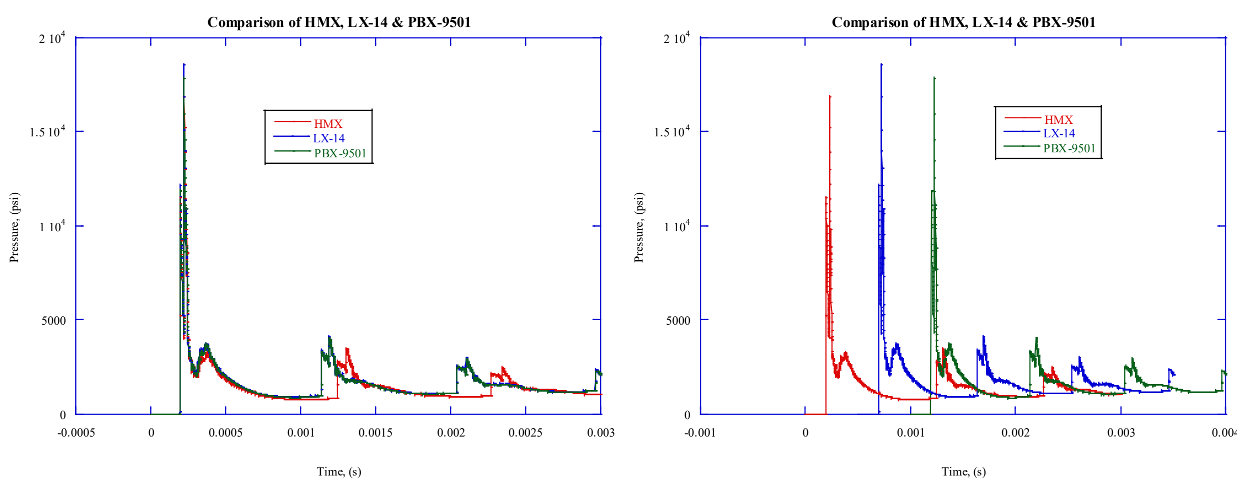

Figure 27 – Detonation results for HMX, LX-14 and PBX-9501 using CTH library EOS parameters.

Additionally, two separate CHEETAH constant-volume explosion analyses were performed for each high-explosive formulation, resulting in peak gas pressure under the following conditions;

(a) vacuum and

(b) partial afterburn.

CHEETAH analyses utilize the internal detonation and combustion variables derived from the thermochemical principles, which are those listed in Table 20 above. Therefore, free-volume quantities of oxidizer and inert gases are included to form a complete set of reactants. From Table 21 two right-most columns, the vacuum and partial afterburn peak gas pressures are listed for all explosives. It is evident, again, that HMX-based explosives LX-14 and PBX-9501 perform similarly on a macro-scale for blast detonations resulting in peak gas pressures that are within 1.5% of each other.

Table 21 – CTH and CHEETAH Results for HMX, LX-14 and PBX-9501

		40-lb HE		CTH 1DS Model								CHEETAH	
				CTH JWL EOS				CHEETAH JWL EOS				Gas Pressure	
HE	Density	HE Diam.		P_r	i_r	t_a	t_p	P_r	i_r	t_a	t_p	#Vacuum	*Afterburn
	(g/cm^3)	(cm)	(in)	(psi)	(psi-ms)	(ms)	(ms)	(psi)	(psi-ms)	(ms)	(ms)	(psi)	(psi)
HMX	1.905	13.150	5.177	16824	1653	0.193	0.225	21466	1834	0.191	0.222	1050	1187
LX-14	1.835	13.315	5.242	18565	1712	0.192	0.223	20740	1817	0.191	0.220	1039	1184
PBX-9501	1.840	13.257	5.219	17808	1717	0.193	0.224	19836	1837	0.190	0.218	1046	1201

Detonation only.
* Partial afterburn per free-volume.

From the foregoing analysis results, it is technically acceptable to use PBX-9501 as the base explosive for all SCE applications where either PBX-9501 or LX-14 are employed in confinement vessels.

6.0 CHEETAH VERIFICATION

Additionally, a significant number of constant-volume explosion calculations were conducted with CHEETAH for the same set of HE's utilized in CTH. The goal with CHEETAH was to determine the amount of TNT that would result in the same peak quasi-static gas pressure as would a 40-lb PBX-9501 charge in a 6-ft ID vessel, with an arbitrary free-volume of 54% (minus the HE-ball), herein referred to the demonstration vessel.

Recall that the CHEETAH solutions provide a TNT-equivalence for peak gas pressures and are generally all less than unity for common explosives relative to TNT. The reason is that TNT has the highest heat-of-combustion among many HE's, thereby resulting in a heat-of-combustion ratio that's lower than 1.0. This methodology would be a correct assumption and would be used in design, if and only if, there is a complete 100% combustion consideration of both explosives, i.e., PBX-9501 and TNT, for example. However, in limited oxygen environments such as confinement vessels, the amount of afterburn (or secondary fireball) will be extremely limited and thus reaction product gas expansion from the detonation process will be predominant in producing quasi-static gas pressure.

Table 22 provides results from constant-volume explosion CHEETAH calculations, with HMX (i.e., similar to PBX-9501) and TNT for the representative 6-ft ID demonstration vessel. Results show that 40-lb of HMX (or PBX-9501) produces a peak gas pressure of 1988 psi (using U1a Drift 05 ambient conditions), whereas a 62-lb TNT charge will produce the same peak gas pressure. This exercise results in a TNT-equivalence of 1.550, which is greater than the standard TNT-equivalence constant of 1.312 for mechanical energy per CHEETAH solution.

Furthermore, Table 7 shows a resulting TNT-equivalence of 1.47 for 40-lb PBX-9501 in the same vessel geometry, whereas 40-lb HMX in Table 22 results in TNT-equivalence of 1.55.

Table 22 – Constant Volume Explosion with CHEETAH

TNT-Equiv for Constant-Volume Explosion with 40-lb HMX CHEETAH

			TNT Mass (lb)	TNT Mass (g)	Air Mass (g)	$V_f/m_{Reactants}$ (cm^3/g)	Gas Pressure (atm)	Gas Pressure (psi)	
HMX	40	(lb)							
Mass	18143.695	(g)							**Note:** 1 atm = 13.2 psi
$Volume_{(Total)}$	113.1	(ft^3)	35	15875.73	70.29	108.455	88.5794	1169	(@ U1a Drift 05)
Free-Volume	61.074	(ft^3)	40	18143.69	70.24	94.951	99.9684	1320	
Free-Volume	1729423.1	(cm^3)	45	20411.66	70.18	84.437	111.3962	1470	
$V_f/m_{Reactants}$	85.64742	(cm^3/g)	50	22679.62	70.12	76.019	122.8635	1622	**TNT-Equivalence**
Pressure	150.4689	(atm)	55	24947.58	70.07	69.128	134.3716	1774	**1.550**
Pressure	**1986**	**(psi)**	60	27215.54	70.01	63.382	145.9175	1926	
			62	**28122.73**	**2018.81**	**57.377**	**150.5466**	**1987**	
			65	29483.50	69.96	58.518	157.5037	2079	

These results require further investigation, and comparison with CTH calculations at extended computational time and possibly different geometries. Table 23 provides an extended listing based on demonstration vessel properties, presenting both UFC-3-340-02 Fig. 2-152 (see Figure 28 in this report) gas pressure and CHEETAH constant-volume explosion calculation with TNT only, at sea level conditions, and thus provides an apples-to-apples comparison without imposing a TNT-equivalence. Figure 29 compares UFC Fig. 2-152 data (i.e., Figure 28 below) for the demonstration vessel with CHEETAH constant-volume explosion calculations utilizing TNT. It is evident that UFC Fig. 2-152 provides consistently conservative peak gas pressures to approximately 150-lb TNT, however it's unknown whether the UFC Fig. 2-152 data is purely based on a detonation or if the peak quasi-static pressure is based on full-combustion as well. Beyond 150-lb, CHEETAH results show higher gas pressures. Thus, if a consistent set of TNT-equivalence value (or values) can be determined for peak quasi-static gas pressure of other explosives such as PBX-9501, then use of Fig. 2-152 is wholly acceptable and encouraged.

Table 23 – Comparison of UFC-3-340-02 with CHEETAH

		Vessel Free-Volume			Gas Pressure			
		1729309.821	(cm^3)					
					Fig. 2-152	CHEETAH		
HE Weight		HE Volume	$(W/V)_{TM-5}$	$(V_f/W_{reactants})$	Sea Level	Sea Level	U1a	$P_{TM-5}/P_{Cheetah}$
(lb)	(g)	(ft^3)	(lb/ft^3)	(cm^3/g)	(psi)	(psi)*	(psi)**	
10	4535.924	0.096846816	0.16401	262.74709	609	474	426	1.28368
15	6803.886	0.145270224	0.24621	195.21183	839	640	574	1.31144
20	9071.847	0.193693632	0.32854	155.24493	1063	806	724	1.31897
25	11339.809	0.24211704	0.41100	128.82734	1277	973	874	1.31249
30	13607.771	0.290540448	0.49359	110.06760	1485	1141	1024	1.30167
35	15875.733	0.338963856	0.57631	96.05748	1666	1310	1176	1.27217
40	18143.695	0.387387264	0.65917	85.19588	1841	1479	1328	1.24462
45	20411.657	0.435810672	0.74216	76.52867	2016	1650	1481	1.22210
50	22679.618	0.48423408	0.82528	69.45184	2188	1821	1635	1.20158
55	24947.580	0.532657488	0.90853	63.56445	2357	1993	1790	1.18256
60	27215.542	0.581080896	0.99192	58.58987	2522	2166	1945	1.16425
65	29483.504	0.629504304	1.07544	54.32941	2695	2340	2101	1.15163
70	31751.466	0.677927712	1.15909	50.64154	2872	2515	2258	1.14194
75	34019.428	0.72635112	1.24288	47.41853	3047	2691	2416	1.13240
80	36287.390	0.774774528	1.32680	44.57693	3221	2867	2575	1.12332
85	38555.351	0.823197936	1.41086	42.05282	3394	3045	2734	1.11459
90	40823.313	0.871621344	1.49506	39.79582	3565	3223	2894	1.10597
95	43091.275	0.920044752	1.57939	37.76564	3734	3403	3056	1.09733
100	45359.237	0.96846816	1.66385	35.92974	3890	3583	3217	1.08565
125	56699.046	1.2105852	2.08823	28.87357	4647	4501	4042	1.03248
130	58967.008	1.259008609	2.17351	28.72214	4795	4687	4209	1.02306
140	63502.932	1.355855425	2.34450	26.62737	5086	5062	4546	1.00473
145	65770.894	1.404278833	2.43021	25.68834	5219	5251	4715	0.99389
150	68038.855	1.452702241	2.51605	24.81191	5351	5441	4886	0.98344
160	72574.779	1.549549057	2.68815	23.22338	5612	5824	5230	0.96358
175	79378.665	1.694819281	2.94736	21.18098	6017	6406	5753	0.93924
200	90718.474	1.936936321	3.38220	18.45778	6898	7397	6642	0.93254

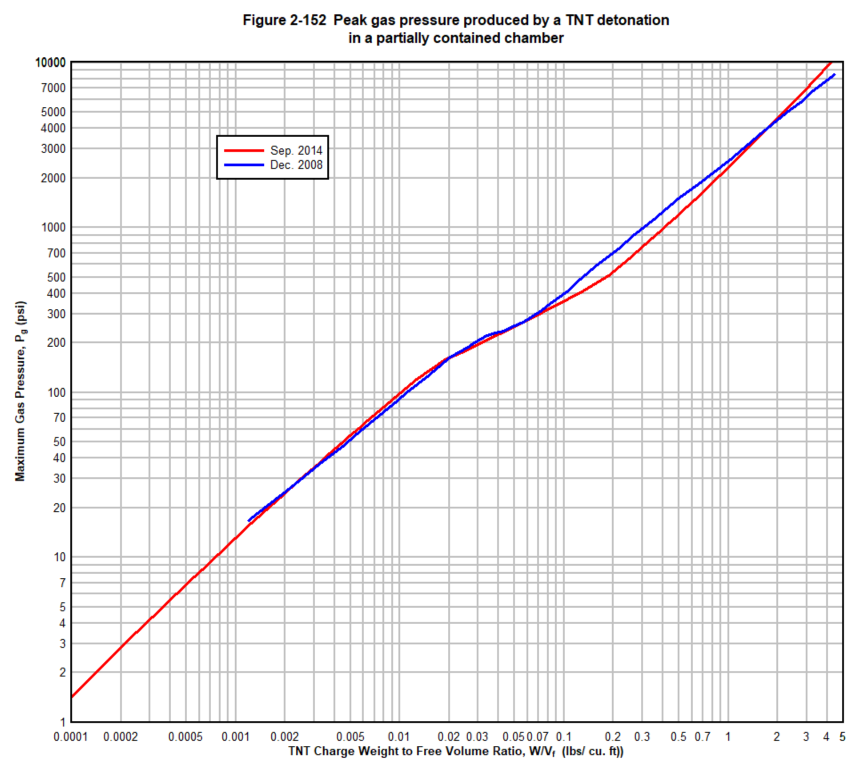

Figure 28 – Peak gas pressure plot from UFC-3-340-02 (Fig. 2-152)

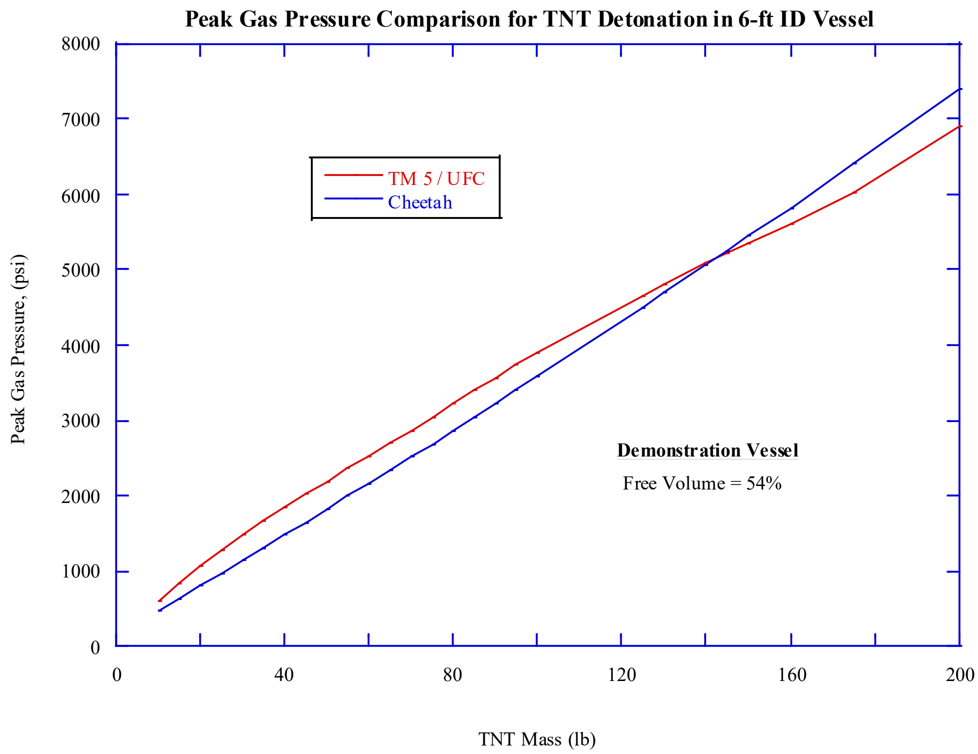

Figure 29 – Peak gas pressure comparison for TNT in 6-ft ID vessel at sea level.

7.0 CONCLUSIONS

LANL (J-2, Dynamic Structure Design and Engineering) has been using a TNT-Equivalence for PBX-9501 in confinement vessel design that appears to be in conflict with the LLNL derived quantities using the thermochemical code CHEETAH. Differences between LANL and LLNL approach to TNT-equivalence has provided an impetus for this investigation. For both TNT and PBX-9501, 1D spherical hydrocode models have been developed under confined constant-volume conditions in 6-ft ID vessels with the use of CTH, as well as application of the thermochemical code CHEETAH.

Although the most widely used methodology for determining TNT-equivalence for HE detonations is the product of the ratio of heat-of-detonation of the HE in question to that of TNT and the mass of HE in question, results of the 1D spherical hydrocode modeling provide a different answer. In other words, the ratio of heat-of-detonation have often been applied to a wide variety of problems, which leads to a constant single-valued (invariant) factor applied to the weight of the HE in question. Results presented herein provide the following conclusions:

1. Peak reflected specific impulse is the key to meaningful scaling of explosives for shock loading in a confined volume.
    a. The structural response of a confinement vessel is directly related to the driving energy supplied during the detonation; i.e., the peak reflected specific impulse.
    b. For the 6-ft ID confinement vessel geometry identified in this study, TNT-equivalence is shown to be approximately 1.188 for a 40-lb PBX-9501 charge.
    c. Both, CTH library JWL EOS and CHEETAH-derived JWL EOS were applied to hydrocode models, showing minor differences in overall results.
2. The importance of proper accounting for incomplete combustion when determining equivalent charge for quasi-static pressure.
    a. As shown in the foregoing analysis, the TNT-equivalence for quasi-static gas pressure without afterburn, i.e., vacuum, is approximately 1.49 for the given vessel geometry and the 40-lb PBX-9501 charge.
    b. CTH hydrocode models and CHEETAH constant-volume explosion calculations results agree within 5%.
3. Using a constant TNT-equivalence conversion factor between PBX-9501 and TNT, for either the shock loading or the quasi-static pressure, is not applicable to confinement vessels, i.e., constant-volume explosion applications.
4. Original differences between LANL and LLNL results for TNT-equivalence were based upon the diverse application of the TNT heat-of-detonation values, where LANL utilized UFC-3-340-02 values and LLNL uses thermochemical principles.
5. Comparison of CTH 1DS analyses for HMX, LX-14 and PBX-9501 for detonation event, and CHEETAH analyses for combustion events, shows minor differences in peak reflected pressure, and particularly peak reflected specific impulse, and peak quasi-static

gas pressure. All three HMX-based high-explosives perform similarly with minor differences.

8.0 RECOMMENDATIONS

The following recommendations are provided for LANL and LLNL project management to consider:

1. It is recommended that LANL and LLNL remove TNT-equivalency methodology for U1a SCE vessel design applications, and instead use PBX-9501 as the base explosive.
    a. For shock loading of the vessel structure, no TNT conversion factors will be utilized, thereby ensuring a one-to-one correspondence.
    b. Likewise, this change should mitigate any further confusion in vessel design, especially ensuring the proper quasi-static gas pressure is applied to o-ring seal and feedthroughs based on the actual explosive.
2. CHEETAH closed-volume explosion calculations shall be used to determine peak quasi-static gas pressures in a confinement vessel.
    a. CHEETAH has the capability of determining the peak quasi-static gas pressure as a function of the available oxidizer in the system (i.e., all reactants), resulting in partial or full-afterburn.
    b. Results can be validated through simple (i.e., less sophisticated) theoretical thermodynamic principles and application of BLAST-X or CONWEP.
3. For zero-room pressurization due to a hypothetical confinement vessel failure, for example a feedthrough blow-out, a combination of CHEETAH calculations and BLAST-X is recommended.
    a. CHEETAH can determine both, the internal gas pressure in the vessel for the given free-volume and an unconfined detonation in the zero-room.
    b. BLAST-X will further determine the rate of pressure increase in the zero-room as a function of time and available heat-transfer mechanisms.
4. For other facility design applications, a TNT-equivalence methodology is fully recommended, as described by J. Maienschein and as shown in UFC-3-340-02, which utilizes the product of the ratio of heat-of-combustion of the explosive in question to that of TNT and the mass of the explosive.
    a. The assumption is that the closed-volume facility is large enough to ensure an abundance of oxidizer (or a stoichiometric mixture) to adequately combust 100% of the reaction product fuels.
        i. Assuming an unconfined detonation in a facility room or drift, an upper-bound solution of peak quasi-static gas pressure is ensured.
    b. The resulting TNT-equivalence factor for PBX-9501 in a large closed-volume is approximately 0.645, given the respective heat-of-combustion of PBX-9501 and TNT.

   c. For this type of analysis, CHEETAH is recommended because it can model the actual mass of reactants (i.e., HE, oxidizer and inert gases) in determining the peak quasi-static pressure for partial or full-afterburn.

5. Based on the CTH and CHEETAH analyses results comparing HMX, LX-14 and PBX-9501, demonstrating similar detonation and combustion performance, LANL recommends using PBX-9501 as the base explosive for SCE applications in confinement vessels involving either LX-14 or PBX-9501.

9.0 REFERENCES

Cooper, P. W., **Explosives Engineering**, VCH Publishers, New York, NY, 1996.

Cooper, P. W., *"Comments on TNT Equivalence,"* SAND94-1614C, Sandia National Laboratories, Presented at 20th International Pyrotechnics Seminar, Colorado Springs, CO, July 24-29, 1994.

Baker, W. E., Cox, P. A., Westine, P. S., Kulesz, J. J., and Strehlow, R. A., **Explosion Hazards and Evaluation**, Elsevier Science, New York, NY, 1983

Kinney, G. F., and Graham, K. J., **Explosive Shocks in Air,** 2nd Edition, Springer-Verlag, New York, NY, 1985.

Locking, P. M., *"The Trouble with TNT Equivalence,"* BAE Systems, Shrivenham, UK, Presented at 26th International Symposium on Ballistics, Miami, FL, Sept. 12-16, 2011.

Xiao, W., Andrae, M. and Gebbeken, N., *"Air Blast TNT Equivalence Concept for Blast-Resistant Design,"* International Journal of Mechanical Science, Vol. 185, June 2020.

King, K. and Vaught, C., *"Determining TNT equivalency for Confined Detonations,"* PVP2008-61699, American Society of Mechanical Engineers, 2008 ASME Pressure Vessel and Piping Division Conference, July 27-31, 2008.

Esparza, E. D., *"Blast Measurements and Equivalency for Spherical Charges at Small Scaled Distances,"* International Journal of Impact Engineering, Vol. 4, No. 1, pp. 23-40, 1986.

Maienschein, J. L., *"Estimating Equivalency of Explosives Through a Thermochemical Approach,"* UCRL-JC-147683, 12th International Conference Symposium, San Diego, CA, August 11-16, 2002.

Dobratz, B. M., *"LLNL Explosives Handbook: Properties of Chemical Explosives and Explosive Simulants,"* UCRL-52997, Lawrence Livermore National Laboratory, March 1981.

Bastea, S., Fried, L. E., et al., *"CHEETAH User's Manual,"* Version 9.0, Lawrence Livermore National Laboratory

United Facilities Criteria, *"Structures to Resist the Effects of Accidental Explosions,"* UFC-3-340-02, US Department of Defense, 5 December 2008.

United Facilities Criteria, *"Design and Analysis of Hardened Structures to Conventional Weapons Effects,"* UFC-3-340-01, US Department of Defense, 1 June 2002.

DOE Manual, *"A Manual for the Prediction of Blast and Fragment Loadings on Structures,"* US Department of Energy, DOE/TIC-11268, July 1992.

DOE O 413.3B, *Program and Project Management for the Acquisition of Capital Assets*, US Department of Energy

DOE-STD-1212, *DOE Technical Standard: Explosives Safety,* US Department of Energy, November 2019.

APPENDIX A

TNT CHARGE: CTH Results

ρ_o	
(g/cm^3)	(lb/in^3)
1.654	0.059755

CHEETAH uses ρ_o = 1.654
CTH uses ρ_o = 1.630
UCRL-52997 uses ρ_o = 1.654

Vessel Inner Radius & Empty -Volume		
(in)	(cm)	(ft^3)
36	91.44	113.0973355

EXCALIBUR Volume	
Percent	(ft^3)
54%	61.07256119

Molecular Weight	
227.132	g/mole

Note: CTH analysis conducted with vessel volume of 113.1 ft^3 minus the HE volume.

						UFC-3-340-02 Blast Curve (Fig. 2-7)												(Fig. 2-152 - 2008)			CTH Analysis - 1D Spherical Model: Reference JWL from CTH					CTH Analysis - 1D Spherical Model: JWL from CHEETAH				
HE Weight		HE Volume		HE Radius		R			Z	P_{so}	P_r	i_r		t_a		U		Free-Vol	W/V_f	P_g	P_r	i_r	t_a	t_{peak}	P_g	P_r	i_r	t_a	t_{peak}	P_g
(lb)	(g)	(in^3)	(cm^3)	(in)	(cm)	(in)	(cm)	(ft)	(ft/lb$^{1/3}$)	(psi)	(psi)	(psi-ms/lb$^{1/3}$)	(psi-ms)	(ms/lb$^{1/3}$)	(ms)	(ft/ms)	(km/s)	(ft^3)	(lb/ft^3)	(psi)	(psi)	(psi-ms)	(ms)	(ms)	(psi)	(psi)	(psi-ms)	(ms)	(ms)	(psi)
10	4535.9	167.3513	2742.4	3.41859	8.68321	32.58141	82.75679	2.71511763	1.260245966	564	4404	162.0803	349.19	0.1183636	0.255007	6.406346	1.95	113.00	0.08850	366										
15	6803.9	251.0269	4113.6	3.91331	9.93980	32.08669	81.50020	2.67389109	1.084209715	737	6099	202.3798	499.11	0.0922998	0.227631	7.265611	2.21	112.95	0.13280	510										
20	9071.8	334.7026	5484.8	4.30715	10.94017	31.69285	80.49983	2.6410707	0.972978765	884	7595	238.2738	646.77	0.0775831	0.210593	7.915362	2.41	112.90	0.17714	645	4997	728	0.262	0.320	580	5748	757	0.258	0.312	685
25	11339.8	418.3782	6856.0	4.63974	11.78494	31.36026	79.65506	2.61335513	0.893754884	1013	8943	271.4304	793.67	0.0679131	0.198579	8.441238	2.57	112.86	0.22152	765	6400	884	0.250	0.301	692					840
30	13607.8	502.0539	8227.2	4.93046	12.52336	31.06954	78.91664	2.58912852	0.8332587	1129	10181	302.669	940.46	0.0609689	0.189445	8.885662	2.71	112.81	0.26594	897	7949	1085	0.241	0.287	834	9150	1110	0.238	0.281	968
35	15875.7	585.7295	9598.4	5.19042	13.18368	30.80958	78.25632	2.56746466	0.784901442	1235	11330	332.4965	1087.62	0.0556894	0.182164	9.271571	2.83	112.76	0.31040	1016	9688	1254	0.234	0.276	910					1125
40	18143.7	669.4052	10969.6	5.42667	13.78374	30.57333	77.65626	2.54777742	0.744974637	1333	12407	361.273	1235.54	0.0515061	0.176148	9.613916	2.93	112.71	0.35489	1131	11246	1459	0.229	0.268	1024	12502	1506	0.226	0.263	1220
45	20411.7	753.0808	12340.8	5.64397	14.33567	30.35603	77.10433	2.52966956	0.711201981	1424	13421	389.085	1383.93	0.048095	0.171069	9.921319	3.02	112.66	0.39943	1247	12608	1610	0.224	0.261	1125					1350
45.08	20447.9	754.4197	12362.7	5.64731	14.34416	30.35269	77.09584	2.52939101	0.71070276	1426	13437	389.5246	1386.32	0.0480454	0.170994	9.926	3.03	112.66	0.40014	1249	13043	1613	0.224	0.260						
50	22679.6	836.7565	13712.0	5.84570	14.84809	30.15430	76.59191	2.51285799	0.682094601	1509	14385	416.2256	1533.39	0.045243	0.166676	10.20151	3.11	112.61	0.44400	1361	15560	1781	0.221	0.255	1245	16929	1882	0.219	0.251	1520
55	24947.6	920.4321	15083.2	6.03440	15.32739	29.96560	76.11261	2.49713299	0.656630084	1590	15305	442.7688	1683.83	0.0428149	0.162823	10.45906	3.19	112.56	0.48861	1472	15542	1949	0.215	0.248	1350					1600
60	27215.5	1004.108	16454.4	6.21199	15.77845	29.78801	75.66155	2.48233437	0.634078748	1666	16185	468.8142	1835.35	0.0407168	0.159401	10.69753	3.26	112.52	0.53326	1573	18454	2105	0.211	0.242	1490	19979	2245	0.209	0.239	1770
62	28122.7	1037.578	17002.9	6.28026	15.95185	29.71974	75.48815	2.47664528	0.625748638	1695	16526	479.1192	1896.30	0.0399548	0.158137	10.78802	3.29	112.50	0.55113	1612										
65	29483.5	1087.783	17825.6	6.37996	16.20510	29.62004	75.23490	2.46833668	0.613903267	1738	17030	494.4373	1988.00	0.0388809	0.156329	10.91966	3.33	112.47	0.57794	1670										
70	31751.5	1171.459	19196.8	6.53952	16.61039	29.46048	74.82961	2.45503962	0.595697566	1807	17844	519.6965	2141.82	0.0372571	0.153547	11.12783	3.39	112.42	0.62267	1764										
75	34019.4	1255.135	20568.0	6.69166	16.99682	29.30834	74.44318	2.44236161	0.579147976	1873	18630	544.6376	2296.83	0.0358078	0.151007	11.32374	3.45	112.37	0.66743	1858										
80	36287.4	1338.81	21939.2	6.83718	17.36643	29.16282	74.07357	2.43023525	0.564007641	1936	19391	569.2955	2453.02	0.0345036	0.148672	11.50896	3.51	112.32	0.71223	1953										
85	38555.4	1422.486	23310.4	6.97675	17.72094	29.02325	73.71906	2.4186042	0.550079121	1997	20130	593.6982	2610.39	0.0333217	0.14651	11.68486	3.56	112.27	0.75708	2047										
90	40823.3	1506.162	24681.6	7.11095	18.06181	28.88905	73.37819	2.40742078	0.537202266	2056	20848	617.8944	2769.03	0.0322451	0.144503	11.85213	3.61	112.23	0.80196	2140										
95	43091.3	1589.837	26052.8	7.24027	18.39028	28.75973	73.04972	2.39664426	0.525245541	2113	21546	641.9181	2929.01	0.0312594	0.142634	12.01143	3.66	112.18	0.84687	2232										
100	45359.2	1673.513	27424.0	7.36513	18.70742	28.63487	72.73258	2.38623953	0.514099723	2168	22227	665.7495	3090.14	0.030351	0.140877	12.16413	3.71	112.13	0.89183	2323										

TNT CHARGE: CTH Results

ρ_o	
(g/cm^3)	(lb/in^3)
1.654	0.059755

CHEETAH uses ρ_o = 1.654
CTH uses ρ_o = 1.630
UCRL-52997 uses ρ_o = 1.654

Dry Air Density	
0.0012041	g/cm^3
0.0011790	g/cm^3 (@ STP)

EXCALIBUR Vessel	
61.07	ft^3
1729309.821	cm^3

CONSTANT-VOLUME EXPLOSION

GENERIC 6-ft ID EMPTY - CHEETAH

						Gas Quantities					No Afterburn (Sea Level)			w/Afterburn (Sea Level)			Vacuum (Sea Level)		
HE Weight		HE Volume		HE Radius		Free-Volume	Air Moles	Mass of Air	Mass O_2	Mass N_2	$V_f/m_{reactant}$	Pressure		$V_f/m_{reactant}$	Pressure		$V_f/m_{reactant}$	Pressure	
(lb)	(g)	(in^3)	(cm^3)	(in)	(cm)	(cm^3)	(mole)	(g)	(g)	(g)	(cm^3/g)	(atm)	(psi)	(cm^3/g)	(atm)	(psi)	(cm^3/g)	(atm)	(psi)
10	4535.9	167.3513	2742.4	3.41859	8.68321	3199817.50	130.78949	3771.97	878.91	2893.06	385.15393	22.19	326.18	385.1539289	23.941072	351.934	705.43901	11.972	175.995
15	6803.9	251.0269	4113.6	3.91331	9.93980	3198446.31	130.73345	3770.35	878.53	2891.82	302.47534	28.23	414.94	302.4753426	30.542746	448.978	470.09114	17.990	264.454
20	9071.8	334.7026	5484.8	4.30715	10.94017	3197075.11	130.67740	3768.74	878.15	2890.58	248.98207	34.28	503.95	248.9820715	37.038553	544.467	352.41721	24.025	353.167
25	11339.8	418.3782	6856.0	4.63974	11.78494	3195703.91	130.62135	3767.12	877.78	2889.34	211.53895	40.35	593.20	211.5389495	43.476021	639.098	281.81285	30.077	442.129
30	13607.8	502.0539	8227.2	4.93046	12.52336	3194332.71	130.56531	3765.50	877.40	2888.10	183.86475	46.44	682.70	183.8647458	49.5542619	728.448	234.74327	36.146	531.339
35	15875.7	585.7295	9598.4	5.19042	13.18368	3192961.51	130.50926	3763.89	877.02	2886.86	162.57756	52.55	772.44	162.5775605	55.233243	811.929	201.12215	42.231	620.796
40	18143.7	669.4052	10969.6	5.42667	13.78374	3191590.31	130.45321	3762.27	876.65	2885.63	145.69503	58.67	862.43	145.6950306	60.952998	896.009	175.90631	48.333	710.501
45	20411.7	753.0808	12340.8	5.64397	14.33567	3190219.12	130.39717	3760.65	876.27	2884.39	131.97824	64.81	952.67	131.9782424	66.704167	980.551	156.29398	54.453	800.452
50	22679.6	836.7565	13712.0	5.84570	14.84809	3188847.92	130.34112	3759.04	875.89	2883.15	120.61309	70.96	1043.16	120.6130851	72.4842	1065.518	140.60413	60.589	890.651
55	24947.6	920.4321	15083.2	6.03440	15.32739	3187476.72	130.28508	3757.42	875.52	2881.91	111.04255	77.14	1133.89	111.0425538	78.29081	1150.875	127.76697	66.741	981.099
60	27215.5	1004.108	16454.4	6.21199	15.77845	3186105.52	130.22903	3755.81	875.14	2880.67	102.87268	83.32	1224.87	102.8726804	84.123349	1236.613	117.06934	72.911	1071.794
62	28122.7	1037.578	17002.9	6.28026	15.95185	3185557.04	130.20661	3755.16	874.99	2880.17	99.93000	85.81	1261.34	99.92999803	86.463385	1271.012	113.27341	75.384	1108.142
65	29483.5	1087.783	17825.6	6.37996	16.20510	3184734.32	130.17298	3754.19	874.76	2879.43	95.81695	89.53	1316.11	95.81694907	89.980674	1322.716	108.01750	79.098	1162.739
70	31751.5	1171.459	19196.8	6.53952	16.61039	3183363.13	130.11694	3752.57	874.39	2878.19	89.66200	95.75	1407.59	89.66200115	95.862093	1409.173	100.25878	85.302	1253.934
75	34019.4	1255.135	20568.0	6.69166	16.99682	3181991.93	130.06089	3750.96	874.01	2876.95	84.24569	101.99	1499.33	84.24568689	101.90419	1497.992	93.53455	91.522	1345.379
80	36287.4	1338.81	21939.2	6.83718	17.36643	3180620.73	130.00484	3749.34	873.63	2875.71	79.44257	108.25	1591.31	79.44257153	108.15579	1589.890	87.65086	97.760	1437.075
85	38555.4	1422.486	23310.4	6.97675	17.72094	3179249.53	129.94880	3747.72	873.26	2874.47	75.15410	114.53	1683.55	75.1541005	114.42707	1682.078	82.45936	104.015	1529.024
90	40823.3	1506.162	24681.6	7.11095	18.06181	3177878.33	129.89275	3746.11	872.88	2873.23	71.30177	120.82	1776.04	71.30176514	120.71645	1774.532	77.84469	110.287	1621.225
95	43091.3	1589.837	26052.8	7.24027	18.39028	3176507.13	129.83670	3744.49	872.50	2871.99	67.82225	127.13	1868.79	67.82225267	127.02365	1867.248	73.71578	116.577	1713.680
100	45359.2	1673.513	27424.0	7.36513	18.70742	3175135.94	129.78066	3742.87	872.13	2870.75	64.66394	133.46	1961.79	64.66393932	133.34854	1960.224	69.99977	122.884	1806.389

APPENDIX B

PBX-9501 CHARGE: CTH Results

ρ_o	
(g/cm^3)	(lb/in^3)
1.859	0.0671606

CHEETAH uses ρ_o = 1.859
CTH uses ρ_o = 1.84
UCRL-52997 uses ρ_o = 1.855

Generic 6-ft ID Vessel		
Ri	91.44	cm

Molecular Weight	
292.87	g/mole

								CTH Analysis - Reference JWL from CTH, 1D Spherical					CTH Analysis - with CHEETAH JWL, 1D Spherical				
Weight		Volume		HE Radius		Vessel Free Vol.		P_r	i_r	t_a	t_{peak}	P_g	P_r	i_r	t_a	t_{peak}	P_g
(lb)	(g)	(in^3)	(cm^3)	(in)	(cm)	(in^3)	(cm^3)	(psi)	(psi-ms)	(ms)	(ms)	(psi)	(psi)	(psi-ms)	(ms)	(ms)	(psi)
10	4535.924	148.896744	2440.0	3.28800	8.35153	195283.3	3200119.92										
15	6803.886	223.345116	3660.0	3.76382	9.56011	195208.9	3198899.929										
20	9071.847	297.793488	4880.0	4.14262	10.52227	195134.4	3197679.939	7318	833	0.222	0.224	785	8232	888	0.218	0.262	
25	11339.809	372.24186	6100.0	4.46251	11.33477	195060	3196459.949					978					
30	13607.771	446.690232	7319.9	4.74212	12.04499	194985.5	3195239.959	12131	1263	0.204	0.241	1152	13560	1369	0.2	0.235	
35	15875.733	521.138604	8539.9	4.99216	12.68008	194911.1	3194019.968					1321					
40	18143.695	595.586976	9759.9	5.21938	13.25722	194836.6	3192799.978	17808	1717	0.193	0.224	1451	19836	1837	0.19	0.218	
45	20411.657	670.035348	10979.9	5.42837	13.78807	194762.2	3191579.988					1678					
50	22679.618	744.48372	12199.9	5.62241	14.28091	194687.7	3190359.998	23373	2117	0.186	0.213	1775	28275	2287	0.183	0.208	
55	24947.580	818.932092	13419.9	5.80390	14.74190	194613.3	3189140.008										
60	27215.542	893.380464	14639.9	5.97470	15.17573	194538.8	3187920.017	27681	2519	0.178	0.203	2070	31056	2744	0.176	0.199	
65	29483.504	967.828836	15859.9	6.13625	15.58608	194464.4	3186700.027										
70	31751.466	1042.277208	17079.9	6.28972	15.97590	194389.9	3185480.037										
75	34019.428	1116.72558	18299.9	6.43605	16.34756	194315.5	3184260.047										
80	36287.390	1191.173952	19519.8	6.57601	16.70305	194241	3183040.056										
85	38555.351	1265.622324	20739.8	6.71025	17.04403	194166.6	3181820.066										
90	40823.313	1340.070696	21959.8	6.83932	17.37188	194092.1	3180600.076										
95	43091.275	1414.519068	23179.8	6.96370	17.68780	194017.7	3179380.086										
100	45359.237	1488.96744	24399.8	7.08379	17.99282	193943.2	3178160.095										

PBX-9501 CHARGE: CTH Results

ρ_o	
(g/cm^3)	(lb/in^3)
1.859	0.0671606

CHEETAH uses ρ_o = 1.859
CTH uses ρ_o = 1.84
UCRL-52997 uses ρ_o = 1.855

Dry Air Density	
0.0012041	g/cm^3
0.0011790	g/cm^3 (@ STP)
28.84	g/mol

EXCALIBUR Vessel	
61.07	ft^3
1729309.821	cm^3

						PBX-9501 Weight			GENERIC 6-ft ID EMPTY VESSEL				
						HMX	ESTANE	BDNPAF					
Weight		Volume		HE Radius		95%	2.50%	2.50%	Volume of Air	Mole Air	Mass of Air	Mass O_2	Mass N_2
(lb)	(g)	(in^3)	(cm^3)	(in)	(cm)	(g)	(g)	(g)	(cm^3)	(mole)	(g)	(g)	(g)
10	4535.924	148.896744	2440.0	3.28800	8.35153	4309.128	113.398	113.398	3200119.920	132.198552	3812.61	888.37427	2924.23196
15	6803.886	223.345116	3660.0	3.76382	9.56011	6463.691	170.097	170.097	3198899.929	132.148153	3811.15	888.03559	2923.11715
20	9071.847	297.793488	4880.0	4.14262	10.52227	8618.255	226.796	226.796	3197679.939	132.097755	3809.70	887.69691	2922.00233
25	11339.809	372.24186	6100.0	4.46251	11.33477	10772.819	283.495	283.495	3196459.949	132.047356	3808.25	887.35823	2920.88752
30	13607.771	446.690232	7319.9	4.74212	12.04499	12927.383	340.194	340.194	3195239.959	131.996958	3806.79	887.01956	2919.77271
35	15875.733	521.138604	8539.9	4.99216	12.68008	15081.946	396.893	396.893	3194019.968	131.94656	3805.34	886.68088	2918.65790
40	18143.695	595.586976	9759.9	5.21938	13.25722	17236.510	453.592	453.592	3192799.978	131.896161	3803.89	886.34220	2917.54308
45	20411.657	670.035348	10979.9	5.42837	13.78807	19391.074	510.291	510.291	3191579.988	131.845763	3802.43	886.00353	2916.42827
50	22679.618	744.48372	12199.9	5.62241	14.28091	21545.638	566.990	566.990	3190359.998	131.795364	3800.98	885.66485	2915.31346
55	24947.580	818.932092	13419.9	5.80390	14.74190	23700.201	623.690	623.690	3189140.008	131.744966	3799.52	885.32617	2914.19865
60	27215.542	893.380464	14639.9	5.97470	15.17573	25854.765	680.389	680.389	3187920.017	131.694567	3798.07	884.98749	2913.08383
65	29483.504	967.828836	15859.9	6.13625	15.58608	28009.329	737.088	737.088	3186700.027	131.644169	3796.62	884.64882	2911.96902
70	31751.466	1042.277208	17079.9	6.28972	15.97590	30163.893	793.787	793.787	3185480.037	131.593771	3795.16	884.31014	2910.85421
75	34019.428	1116.72558	18299.9	6.43605	16.34756	32318.456	850.486	850.486	3184260.047	131.543372	3793.71	883.97146	2909.73939
80	36287.390	1191.173952	19519.8	6.57601	16.70305	34473.020	907.185	907.185	3183040.056	131.492974	3792.26	883.63278	2908.62458
85	38555.351	1265.622324	20739.8	6.71025	17.04403	36627.584	963.884	963.884	3181820.066	131.442575	3790.80	883.29411	2907.50977
90	40823.313	1340.070696	21959.8	6.83932	17.37188	38782.148	1020.583	1020.583	3180600.076	131.392177	3789.35	882.95543	2906.39496
95	43091.275	1414.519068	23179.8	6.96370	17.68780	40936.711	1077.282	1077.282	3179380.086	131.341779	3787.90	882.61675	2905.28014
100	45359.237	1488.96744	24399.8	7.08379	17.99282	43091.275	1133.981	1133.981	3178160.095	131.29138	3786.44	882.27808	2904.16533

	CONSTANT-VOLUME EXPLOSION - GENERIC 6-FT ID VESSEL								
	CHEETAH (Vacuum) (Sea Level Conditions)			CHEETAH (Conservative) (Sea Level Conditions)			CHEETAH (w/Afterburn) (Sea Level Conditions)		
Weight	$V_f/m_{reactant}$	Pressure		$V_f/m_{reactant}$	Pressure		$V_f/m_{reactant}$	Pressure	
(lb)	(cm^3/g)	(atm)	(psi)	(cm^3/g)	(atm)	(psi)	(cm^3/g)	(atm)	(psi)
10	705.5056768	17.04660	250.585	383.3153798	32.10	471.90	383.3153798	26.486509	389.3516823
15	470.15781	25.88686	380.537	301.3554773	41.08	603.83	301.3554773	35.725228	525.1608516
20	352.4838766	34.82100	511.869	248.2372674	50.12	736.71	248.2372674	44.896443	659.9777121
25	281.8795166	43.82831	644.276	211.0145459	59.21	870.40	211.0145459	54.066431	794.7765357
30	234.8099432	52.89685	777.584	183.4809114	68.35	1004.81	183.4809114	63.256787	929.8747689
35	201.1888194	62.01891	911.678	162.2889248	77.54	1139.90	162.2889248	72.475718	1065.393055
40	175.9729765	71.18913	1046.480	145.4738958	86.78	1275.59	145.4738958	81.726431	1201.378536
45	156.3606543	80.40355	1181.932	131.806737	96.05	1411.87	131.806737	91.010031	1337.847456
50	140.6707965	89.65919	1317.990	120.4791577	105.35	1548.70	120.4791577	100.32659	1474.800873
55	127.8336401	98.95370	1454.619	110.9377793	114.70	1686.06	110.9377793	109.67588	1612.235436
60	117.1360098	108.28519	1591.792	102.7909893	124.08	1823.92	102.7909893	119.05736	1750.143192
65	108.0841688	117.65214	1729.486	95.75385686	133.49	1962.27	95.75385686	128.47052	1888.516644
70	100.3254479	127.05327	1867.683	89.61412137	142.93	2101.10	89.61412137	137.91485	2027.348295
75	93.60122311	136.48751	2006.366	84.21041374	152.41	2240.39	84.21041374	147.38977	2166.629619
80	87.71752644	145.95396	2145.523	79.41786661	161.19	2369.55	79.41786661	156.89485	2306.354295
85	82.52602938	155.45183	2285.142	75.1383459	171.45	2520.33	75.1383459	166.42958	2446.514826
90	77.91136532	164.98047	2425.213	71.29365999	181.02	2660.96	71.29365999	175.99359	2587.105773
95	73.78245538	174.53929	2565.728	67.82073887	190.61	2802.02	67.82073887	185.58651	2728.121697
100	70.06643643	184.12779	2706.679	64.66814722	200.22	2943.29	64.66814722	195.20797	2869.557159

APPENDIX C

CHEETAH RESULTS - TNT

ρ_o	M_w	ΔH_f		$(\Delta H_d)_{Mech}$	$(\Delta H_d)_{Total}$	(ΔH_c)		D_{C-J}	P_{C-J}	c_s
(g/cm^3)	(g/mol)	(cal/g)	(kJ/g)	(kJ/g)	(kJ/g)	(cal/g)	(kJ/g)	(km/s)	(GPa)	(km/s)
1.654	227.132	-66.504	-0.278253	-4.3464	-4.4621	3472.5	14.52894	7.20971	21.49	5.52135

Note: P_{C-J} was estimated using:

$$P_{C-J} = \frac{\rho_o D_{C-J}^2}{4}$$

CHEETAH JWL PARAMETERS - TNT

ρ_o	T_o		v_o	A	B	C	R1	R2	ω	T_{C-J}		E_o	D_{C-J}	P_{C-J}	
(g/cm^3)	(eV)	(K)	(cm^3/g)	(GPa)	(GPa)	(GPa)				(eV)	(K)	(kJ/cm^3)	(km/s)	(dyn/cm^2)	(GPa)
1.654	0.02568	298.00	0.6045949	1594.00	50.80	1.536	6.732	2.302	0.38778	0.350	4062	-7.189	7.20971	2.15E+11	21.49

CTH JWL PARAMETERS - TNT

ρ_o	T_o		v_o	AG	BG	R1	R2	WG	CV	T_{C-J}		E_o	D_{C-J}	P_{C-J}	
(g/cm^3)	(eV)	(K)	(cm^3/g)	(dyn/cm^2)	(dyn/cm^2)				(erg/g/eV)	(eV)	(K)	(dyn/cm^2)	(cm/s)	(dyn/cm^2)	(GPa)
1.63	0.02568	298.00	0.6134969	3.71E+12	3.23E+10	4.15	0.95	0.3	6.724E+10	0.350	4062	7.01E+10	6.93E+05	2.10E+11	21.01

Note: WG is ω

Unit Conversions					
1	eV	1	GPa	1	erg
11604.53	K	1.00E+10	dyn/cm^2	1	dyn-cm

JWL form in CHEETAH

$$P = A\exp\left[-R_1\frac{v}{v_o}\right] + B\exp\left[-R_2\frac{v}{v_o}\right] + C\left(\frac{v}{v_o}\right)^{-(1+\omega)}$$

JWL form in CTH

$$P(\rho,T) = A\exp\left(-R_1\frac{\rho_o}{\rho}\right) + B\exp\left(-R_2\frac{\rho_o}{\rho}\right) + \omega\rho C_V T$$

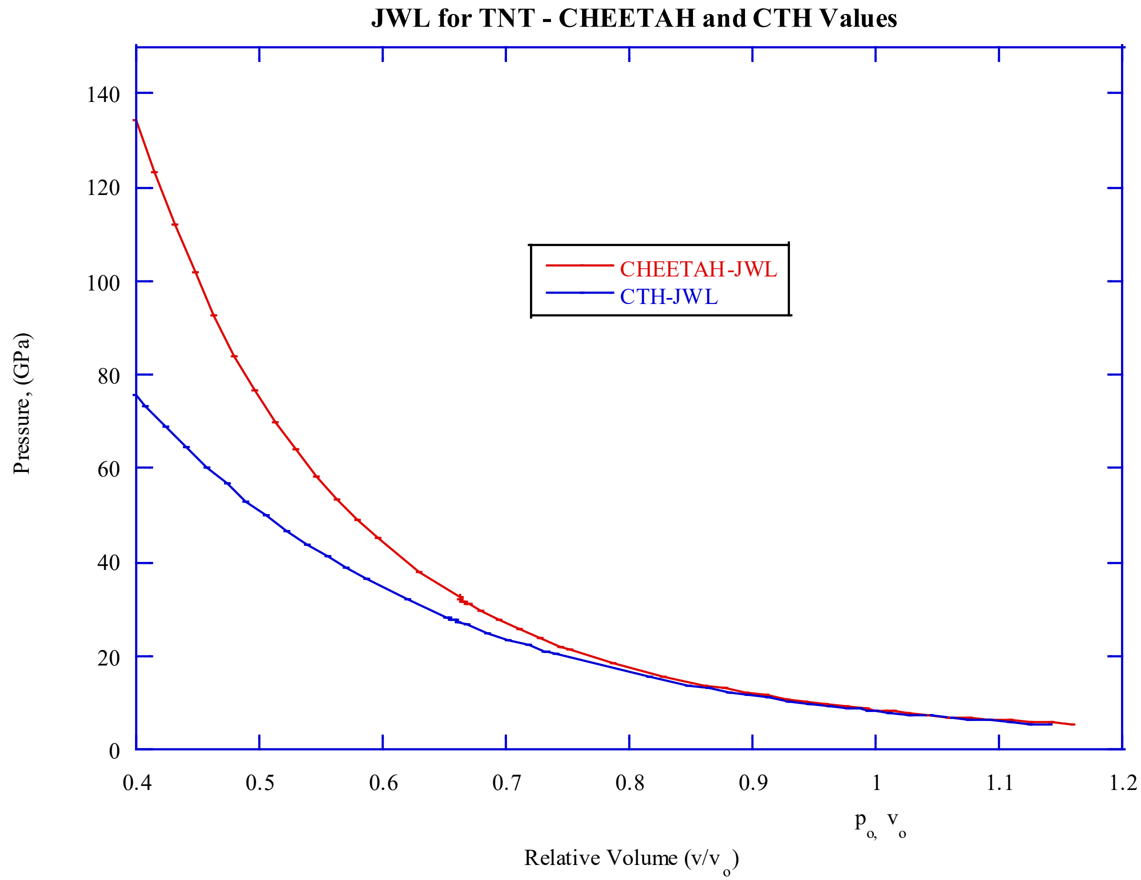

Figure 30 – Comparison of TNT JWL EOS's between CTH and CHEETAH.

The JWL EOS in CHEETAH for TNT, developed from thermochemical principles, matches quite well with the CTH JWL EOS over a narrow range of reaction product specific volume. Below a specific volume of ~0.5 cm^3/g, the respective EOS diverge greatly. Certainly

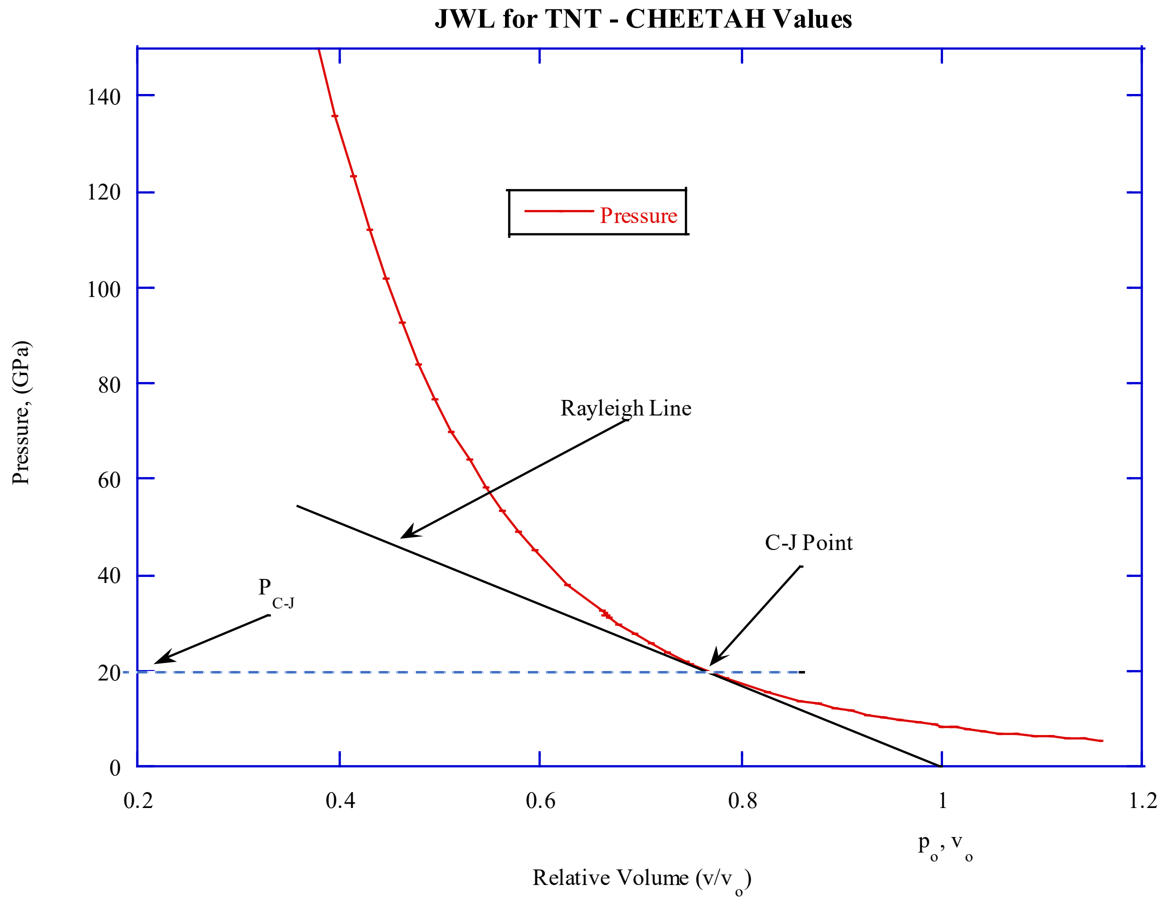

Figure 31 – CHEETAH JWL EOS and C-J point.

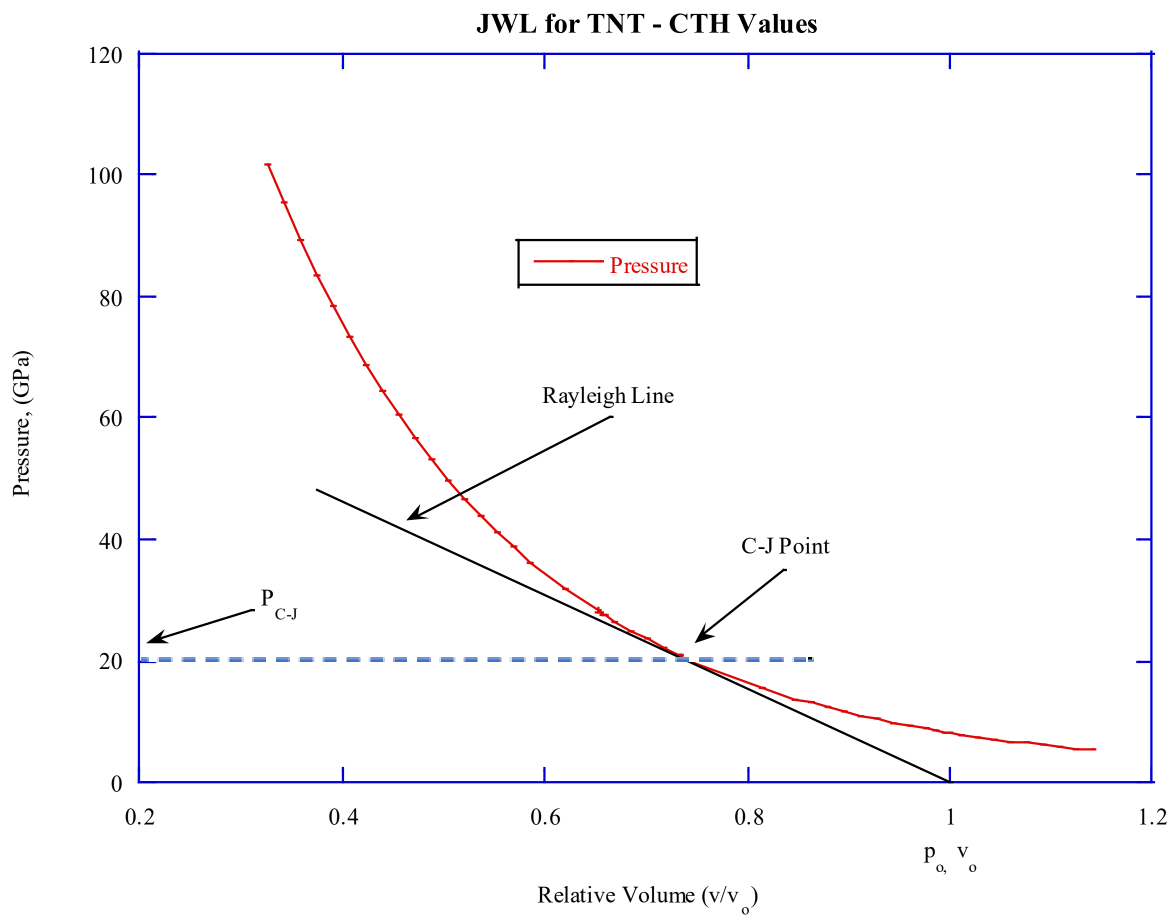

Figure 32 – CTH JWL EOS and C-J point.

APPENDIX D

CHEETAH RESULTS - PBX-9501

ρ_o	M_w	ΔH_f		$(\Delta H_d)_{Mech}$	$(\Delta H_d)_{Total}$	(ΔH_c)		D_{C-J}	P_{C-J}	c_s
(g/cm^3)	(g/mol)	(cal/g)	(kJ/g)	(kJ/g)	(kJ/g)	(cal/g)	(kJ/g)	(km/s)	(GPa)	(km/s)
1.8592	292.87	27.286	0.1141646	-5.7022	-5.7022	2239.5	9.370068	8.90935	36.8942053	6.77642

Note: P_{C-J} was estimated using:

$$P_{C-J} = \frac{\rho_o D_{C-J}^2}{4}$$

CHEETAH JWL PARAMETERS - PBX-9501

ρ_o	T_o		v_o	A	B	C	R1	R2	ω	T_{C-J}		E_o	D_{C-J}	P_{C-J}	
(g/cm^3)	(eV)	(K)	(cm^3/g)	(GPa)	(GPa)	(GPa)				(eV)	(K)	(kJ/cm^3)	(km/s)	(dyn/cm^2)	(GPa)
1.8592	0.0256798	298.00	0.5378657	3570.00	112.20	2.352	7.377	2.356	0.5308	0.350	4062	-10.60	8.90935	3.69E+11	36.89

CTH JWL PARAMETERS - PBX-9501

ρ_o	T_o		v_o	AG	BG	R1	R2	WG	CV	T_{C-J}		E_o	D_{C-J}	P_{C-J}	
(g/cm^3)	(eV)	(K)	(cm^3/g)	(dyn/cm^2)	(dyn/cm^2)				(erg/g/eV)	(eV)	(K)	(dyn/cm^2)	(cm/s)	(dyn/cm^2)	(GPa)
1.84	0.0256798	298.00	0.5434783	8.52E+12	1.80E+11	4.6	1.3	0.38	5.527E+10	0.350	4062	1.02E+11	8.80E+05	3.70E+11	37.00

Note: WG is ω

Unit Conversions					
1	eV	1	GPa	1	erg
11604.53	K	1.00E+10	dyn/cm^2	1	dyn-cm

JWL form in CHEETAH

$$P = A\exp\left[-R_1\frac{v}{v_o}\right] + B\exp\left[-R_2\frac{v}{v_o}\right] + C\left(\frac{v}{v_o}\right)^{-(1+\omega)}$$

JWL form in CTH

$$P(\rho,T) = A\exp\left(-R_1\frac{\rho_o}{\rho}\right) + B\exp\left(-R_2\frac{\rho_o}{\rho}\right) + \omega\rho C_V T$$

APPENDIX E

CHEETAH RESULTS - HMX

ρ_o	M_w	ΔH_f		$(\Delta H_d)_{Mech}$	$(\Delta H_d)_{Total}$	(ΔH_c)		$D_{C\text{-}J}$	$P_{C\text{-}J}$	c_s
(g/cm³)	(g/mol)	(cal/g)	(kJ/g)	(kJ/g)	(kJ/g)	(cal/g)	(kJ/g)	(km/s)	(GPa)	(km/s)
1.905	296.156	60.527	0.253245	-5.8677	-5.8677	2115.7	8.852089	9.18856	40.2096136	7.01856

Note: $P_{C\text{-}J}$ was estimated using:

$$P_{C-J} = \frac{\rho_o D_{C-J}^2}{4}$$

CHEETAH JWL PARAMETERS - HMX

ρ_o	T_o		v_o	A	B	C	R1	R2	ω	$T_{C\text{-}J}$		E_o	$D_{C\text{-}J}$	$P_{C\text{-}J}$	
(g/cm³)	(eV)	(K)	(cm³/g)	(GPa)	(GPa)	(GPa)				(eV)	(K)	(kJ/cm³)	(km/s)	(dyn/cm²)	(GPa)
1.905	0.02568	298.00	0.524934	4437.00	122.60	2.548	7.543	2.364	0.56	0.350	4062	-11.18	9.11886	3.96E+11	39.60191

CTH JWL PARAMETERS - HMX

ρ_o	T_o		v_o	AG	BG	R1	R2	WG	CV	$T_{C\text{-}J}$		E_o	$D_{C\text{-}J}$	$P_{C\text{-}J}$	
(g/cm³)	(eV)	(K)	(cm³/g)	(dyn/cm²)	(dyn/cm²)				(erg/g/eV)	(eV)	(K)	(dyn/cm²)	(km/s)	(dyn/cm²)	(GPa)
1.891	0.02568	298.00	0.528821	7.78E+12	7.07E+10	4.20	1.00	0.30	9.909E+10	0.350	4062	1.29E+11	9.110	4.15E+11	41.50

Note: WG is ω

Unit Conversions					
1	eV	1	GPa	1	erg
11604.53	K	1.00E+10	dyn/cm²	1	dyn-cm

JWL form in CHEETAH

$$P = A\exp\left[-R_1\frac{v}{v_o}\right] + B\exp\left[-R_2\frac{v}{v_o}\right] + C\left(\frac{v}{v_o}\right)^{-(1+\omega)}$$

JWL form in CTH

$$P(\rho,T) = A\exp\left(-R_1\frac{\rho_o}{\rho}\right) + B\exp\left(-R_2\frac{\rho_o}{\rho}\right) + \omega\rho C_V T$$

APPENDIX F

CHEETAH RESULTS - LX-14

ρ_o	M_w	ΔH_f		$(\Delta H_d)_{Mech}$	$(\Delta H_d)_{Total}$	(ΔH_c)		D_{C-J}	P_{C-J}	c_s
(g/cm^3)	(g/mol)	(cal/g)	(kJ/g)	(kJ/g)	(kJ/g)	(cal/g)	(kJ/g)	(km/s)	(GPa)	(km/s)
1.85375	289.373	15.108	0.063212	-5.6169	-5.6169	2292.8	9.593075	8.85201	34.853	6.728

Note: P_{C-J} was estimated using:

$$P_{C-J} = \frac{\rho_o D_{C-J}^2}{4}$$

CHEETAH JWL PARAMETERS - LX-14

ρ_o	T_o		v_o	A	B	C	R1	R2	ω	T_{C-J}		E_o	D_{C-J}	P_{C-J}	
(g/cm^3)	(eV)	(K)	(cm^3/g)	(GPa)	(GPa)	(GPa)				(eV)	(K)	(kJ/cm^3)	(km/s)	(dyn/cm^2)	(GPa)
1.85375	0.0256798	298.00	0.539447	3281.00	110.30	2.251	7.268	2.36	0.51701	0.350	4062	-10.41	8.85201	3.485E+11	34.853
				(dyn/cm2)	(dyn/cm2)	(dyn/cm2)									
				3.2810E+13	1.1030E+12	2.2510E+10									

CTH JWL PARAMETERS - LX-14

ρ_o	T_o		v_o	AG	BG	R1	R2	WG	CV	T_{C-J}		E_o	D_{C-J}	P_{C-J}	
(g/cm^3)	(eV)	(K)	(cm^3/g)	(dyn/cm^2)	(dyn/cm^2)				(erg/g/eV)	(eV)	(K)	(dyn/cm^2)	(cm/s)	(dyn/cm^2)	(GPa)
1.835	0.0256798	298.00	0.544959	8.261E+12	1.724E+11	4.55	1.32	0.38	5.527E+10	0.350	4062	1.02E+11	8.80E+05	3.700E+11	37.00

Note: WG is ω

Unit Conversions					
1	eV	1	GPa	1	erg
11604.53	K	1.00E+10	dyn/cm^2	1	dyn-cm

APPENDIX G

ZERO-ROOM PEAK GAS PRESSURES UNDER DETONATION AND FULL-COMBUSTION FOR PBX-9501 AND TNT

Zero-Room Volume	
100000	ft^3
2831684659	cm^3

PBX-9501 - ρ_o	
(g/cm^3)	(lb/in^3)
1.859	0.06716064

Dry Air Density	
0.0012041	g/cm^3
0.0011790	g/cm^3 (@ STP)
28.84	g/mole

Mw (N_2)	
28	g/mole
Mw (O_2)	
32	g/mole

PBX-9501								PBX-9501 Weight			Empty Room							CHEETAH				
								HMX	ESTANE	BDNPAF												
Weight		Volume		HE Radius		Room Free Vol.		95%	2.50%	2.50%	Volume of Air	Moles of Air	Mass of Air	Moles O_2	Mass O_2	Moles N_2	Mass N_2	$V_f/m_{reactant}$	Pressure		Increase	
(lb)	(g)	(in^3)	(cm^3)	(in)	(cm)	(ft^3)	(cm^3)	(g)	(g)	(g)	(cm^3)	(mole)	(g)	(mole)	(g)	(mole)	(g)	(cm^3/g)	(atm)	(psi)	(psi)	
0.001	0.5	0.01488967	0.2	0.15262	0.38764	99999.99999	2831684659.0	0.43091	0.01134	0.01134	2831684659.0	115742.4	3338011.20	24305.91	777789.018	91436.51	2560222.184	848.3148	1.0109359	13.34435	0.14435	
10	4535.9	148.896744	2440.0	3.28800	8.35153	99999.91383	2831682219.2	4309.128	113.398	113.398	2831682219.2	115742.3	3338008.33	24305.89	777788.348	91436.43	2560219.979	847.1637	1.0700294	14.12439	0.92439	
15	6803.9	223.345116	3660.0	3.76382	9.56011	99999.87075	2831680999.2	6463.691	170.097	170.097	2831680999.2	115742.3	3338006.89	24305.88	777788.013	91436.39	2560218.876	846.5893	1.0994786	14.51312	1.31312	
20	9071.8	297.793488	4880.0	4.14262	10.52227	99999.82767	2831679779.2	8618.255	226.796	226.796	2831679779.2	115742.2	3338005.45	24305.86	777787.678	91436.35	2560217.773	846.0157	1.1288615	14.90097	1.70097	
25	11339.8	372.24186	6100.0	4.46251	11.33477	99999.78458	2831678559.2	10772.819	283.495	283.495	2831678559.2	115742.2	3338004.01	24305.85	777787.343	91436.31	2560216.670	845.4428	1.1581782	15.28795	2.08795	
30	13607.8	446.690232	7319.9	4.74212	12.04499	99999.7415	2831677339.3	12927.383	340.194	340.194	2831677339.3	115742.1	3338002.57	24305.84	777787.008	91436.27	2560215.567	844.8707	1.1874293	15.67407	2.47407	
35	15875.7	521.138604	8539.9	4.99216	12.68008	99999.69842	2831676119.3	15081.946	396.893	396.893	2831676119.3	115742.1	3338001.14	24305.83	777786.672	91436.23	2560214.463	844.2994	1.2166151	16.05932	2.85932	
40	18143.7	595.586976	9759.9	5.21938	13.25722	99999.65533	2831674899.3	17236.510	453.592	453.592	2831674899.3	115742.0	3337999.70	24305.82	777786.337	91436.19	2560213.360	843.7288	1.2457359	16.44371	3.24371	6-ft ID Vessel Limit
45	20411.7	670.035348	10979.9	5.42837	13.78807	99999.61225	2831673679.3	19391.074	510.291	510.291	2831673679.3	115742.0	3337998.26	24305.81	777786.002	91436.15	2560212.257	843.1590	1.2747922	16.82726	3.62726	
50	22679.6	744.48372	12199.9	5.62241	14.28091	99999.56916	2831672459.3	21545.638	566.990	566.990	2831672459.3	115741.9	3337996.82	24305.80	777785.667	91436.11	2560211.154	842.5900	1.3037842	17.20995	4.00995	
55	24947.6	818.932092	13419.9	5.80390	14.74190	99999.52608	2831671239.3	23700.201	623.690	623.690	2831671239.3	115741.9	3337995.38	24305.79	777785.332	91436.07	2560210.051	842.0218	1.3327126	17.59181	4.39181	
60	27215.5	893.380464	14639.9	5.97470	15.17573	99999.483	2831670019.3	25854.765	680.389	680.389	2831670019.3	115741.8	3337993.95	24305.78	777784.997	91436.03	2560208.948	841.4543	1.3615773	17.97282	4.77282	
65	29483.5	967.828836	15859.9	6.13625	15.58608	99999.43991	2831668799.3	28009.329	737.088	737.088	2831668799.3	115741.8	3337992.51	24305.77	777784.662	91435.99	2560207.845	840.8876	1.3903791	18.35300	5.15300	
70	31751.5	1042.27721	17079.9	6.28972	15.97590	99999.39683	2831667579.3	30163.893	793.787	793.787	2831667579.3	115741.7	3337991.07	24305.76	777784.327	91435.96	2560206.742	840.3216	1.4191183	18.73236	5.53236	
75	34019.4	1116.72558	18299.9	6.43605	16.34756	99999.35375	2831666359.3	32318.456	850.486	850.486	2831666359.3	115741.7	3337989.63	24305.75	777783.992	91435.92	2560205.639	839.7565	1.447796	19.11091	5.91091	
80	36287.4	1191.17395	19519.8	6.57601	16.70305	99999.31066	2831665139.4	34473.020	907.185	907.185	2831665139.4	115741.6	3337988.19	24305.74	777783.657	91435.88	2560204.536	839.1920	1.4764099	19.48861	6.28861	
85	38555.4	1265.62232	20739.8	6.71025	17.04403	99999.26758	2831663919.4	36627.584	963.884	963.884	2831663919.4	115741.6	3337986.75	24305.73	777783.321	91435.84	2560203.433	838.6283	1.5087889	19.91601	6.71601	
90	40823.3	1340.0707	21959.8	6.83932	17.37188	99999.2245	2831662699.4	38782.148	1020.583	1020.583	2831662699.4	115741.5	3337985.32	24305.72	777782.986	91435.80	2560202.330	838.0654	1.5334554	20.24161	7.04161	
95	43091.3	1414.51907	23179.8	6.96370	17.68780	99999.18141	2831661479.4	40936.711	1077.282	1077.282	2831661479.4	115741.5	3337983.88	24305.71	777782.651	91435.76	2560201.227	837.5033	1.5618867	20.61690	7.41690	
100	45359.2	1488.96744	24399.8	7.08379	17.99282	99999.13833	2831660259.4	43091.275	1133.981	1133.981	2831660259.4	115741.4	3337982.44	24305.70	777782.316	91435.72	2560200.124	836.9419	1.5902577	20.99140	7.79140	

$$PV = nRT \qquad \frac{V}{n} = \frac{RT}{P}$$

R	82.05736	cm^3-atm/mole-K
T	298.15	K
P	1	atm (@ sea level)

Specific Volume Air	
24465.40	cm^3/mole

R	82.05736	cm^3-atm/mole-K
T	298.15	K
P	0.89821	atm (@ U1a 05 Drift)

Specific Volume Air	
27238.05	cm^3/mole

APPENDIX H

HE Data Derived from CTH Library

HE	Composition	Density (g/cm^3)	Mw (g/mol)	ΔH_f (kJ/g)	ΔH_d (kJ/g)	ΔH_c (kJ/g)	$P_{C\text{-}J}$ (GPa)	$D_{C\text{-}J}$ (km/s)
TNT	100% TNT	1.63	227.1	0.284	4.56	14.98	21.01	6.93
HMX	100% HMX	1.905	296.2	0.253	6.78	9.43	41.50	9.11
LX-14	95.5% HMX 4.5% Estane	1.835	289.4	0.0628	6.59	9.593*	37.00	8.80
PBX-9501	95% HMX 2.5% Estane 2.5% BDNPA-F	1.84	292.9	0.0954	6.65	9.40	37.00	8.80
						*Cheetah		

HE Data Derived from CHEETAH

HE	Composition	Density (g/cm^3)	Mw (g/mol)	ΔH_f (kJ/g)	ΔH_d (kJ/g)	ΔH_c (kJ/g)	$P_{C\text{-}J}$ (GPa)	$D_{C\text{-}J}$ (km/s)
TNT	100% TNT	1.654	227.132	0.2783	4.3464	14.53	21.49	7.21
HMX	100% HMX	1.905	296.156	0.2532	5.8677	8.852	39.6	9.19
LX-14	95.5% HMX 4.5% Estane	1.85375	289.373	0.0632	5.6169	9.593	34.853	8.85
PBX-9501	95% HMX 2.5% Estane 2.5% BDNPA-F	1.8592	292.87	0.1142	5.7022	9.37	36.89	8.91